geosciences

MDPI

Article

Characteristics and Formation Mechanisms of Cambrian Platform-Margin High-Energy Shoal Reservoirs in the Yudu Area, Tarim Basin

Yang Liu [1,4], Junhui Li [1], Ran Xiong [2,4,*], Bo Yan [1], Rui Deng [1], Yuangao Zhang [3], Xiandong Wang [1], Yong Zhong [1], Yanqing Cao [3] and Shan Zhao [1]

[1] Exploration and Development Research Institute, PetroChina Daqing Oilfield Company Limited, Daqing 163435, China; liuyang521927@petrochina.com.cn (Y.L.)
[2] Petrochina Hangzhou Research Institute of Geology, Hangzhou 310023, China
[3] Xinjiang Branch, PetroChina Daqing Oilfield Company Limited, Daqing 163435, China
[4] State Key Laboratory of Oil and Gas Reservoir Geology and Exploitation, Southwest Petroleum University, Chengdu 610500, China
* Correspondence: xiongr_hz@petrochina.com.cn

Abstract

The Cambrian platform-margin shoals in the Yudu area, Tarim Basin, are important targets for deep and ultra-deep hydrocarbon exploration, but their development and reservoir-forming mechanisms remain poorly constrained. This study integrates 3D seismic interpretation, drilling and logging data, core observations, thin-section petrography, and reservoir characterization to investigate shoal architecture, reservoir characteristics, and controlling processes. Seismic data reveal that multistage, basinward-prograding carbonate buildups developed along fault-controlled platform-margin slope breaks adjacent to the Yudu rift trough. Core and petrographic observations show that the shoals are dominated by granular, microbial, algal, and oolitic dolomites, with intercrystalline, dissolution, vuggy, and fracture-related pore systems. High-quality reservoirs are preferentially developed within thick, vertically stacked shoal complexes and are characterized by strong heterogeneity and locally enhanced porosity and permeability. Early dolomitization favored the preservation of primary pore frameworks, whereas subsequent faulting and multistage dissolution generated and enhanced fracture–vuggy reservoir space. The spatial association between platform-margin shoals and the Yudu rift trough further provided favorable conditions for near-source hydrocarbon accumulation. These results demonstrate that Cambrian reservoir development was governed by coupled tectono-sedimentary and diagenetic processes and highlight fault-controlled platform margins as favorable targets for deep and ultra-deep carbonate exploration.

Keywords: Tarim Basin; Yudu area; Cambrian; platform-margin shoals; dolomite reservoirs; tecto-karstification; fault-controlled reservoirs; ultra-deep carbonates

Check for updates

Academic Editor: Michele Morsilli

Received: 22 July 2026
Revised: 7 September 2026
Accepted: 8 September 2026
Published: 13 September 2026

Copyright: © 2026 by the authors. Licensee MDPI, Basel, Switzerland. This article is an open access article distributed under the terms and conditions of the Creative Commons Attribution (CC BY) license.

1. Introduction

Deep and ultra-deep carbonate reservoirs in the Tarim Basin have become one of the most important targets for hydrocarbon exploration in China during the past decade [1–3]. In particular, the Cambrian subsalt dolomite system in the Tarim Basin contains abundant hydrocarbon resources and exhibits significant exploration potential [4,5]. Recent exploration breakthroughs in the Shunbei, Tazhong, and northern Tarim regions demonstrate

that platform-margin carbonate buildups and associated dolomite reservoirs constitute the primary exploration targets in the deep Cambrian succession [5–7]. The discovery of high-productivity reservoirs in deeply buried Cambrian strata indicates that favorable reservoirs can still be preserved under ultra-deep burial conditions (>7000 m), despite intense compaction and complex tectono-diagenetic modifications.

Previous studies have shown that the development of high-quality Cambrian carbonate reservoirs in the Tarim Basin is closely related to the evolution of rift-controlled paleogeomorphology, platform-margin facies belts, dolomitization, and multi-stage karstification [8–10]. Synsedimentary extensional tectonism during the Early–Middle Cambrian resulted in the formation of a series of intracratonic rift troughs and fault-controlled platform margins in the Tarim Basin [11–13]. These paleogeomorphic highs and slope-break zones provided favorable conditions for the development of high-energy shoal complexes, microbial buildups, and platform-margin reef–shoal systems [14–16]. In recent years, increasing attention has been paid to the controlling effects of Cambrian rift troughs on source rock distribution, sedimentary facies differentiation, and hydrocarbon accumulation [17–20]. In particular, the coupling relationship between rift troughs and platform-margin shoal reservoirs has become a major focus in deep carbonate exploration.

The Yudu area, located in the western slope-break zone of the Tarim Basin, is situated adjacent to the Yudu rift trough and represents an important exploration domain for deep Cambrian dolomite reservoirs [8,21,22]. Seismic interpretation and drilling data indicate that the Cambrian platform margin in this area was strongly controlled by synsedimentary fault activity and inherited paleogeomorphology [23–25]. Multiple stages of platform-margin shoals developed along the slope-break belt, forming large-scale shoal complexes characterized by progradational geometries and lateral migration [14,26,27]. Recent exploration results from the study area reveal the presence of thick dolomite reservoirs with abundant dissolution pores, vugs, and fractures, indicating favorable reservoir quality in the platform-margin shoal belts [28–30]. Moreover, hydrocarbon shows, overflow phenomena, and high-pressure coefficients observed in several wells suggest that the platform-margin reservoirs adjacent to hydrocarbon kitchens possess excellent hydrocarbon accumulation conditions [31,32].

Although significant progress has been achieved in the exploration of Cambrian carbonate reservoirs in the Tarim Basin, several key issues remain unresolved in the Yudu area. First, the spatial distribution and evolutionary characteristics of platform-margin high-energy shoals are still poorly constrained due to limited drilling penetration and the complexity of deep seismic responses. Second, the coupling relationship between synsedimentary fault-controlled paleogeomorphology and shoal development remains unclear. Third, the formation mechanisms of high-quality dolomite reservoirs, particularly the relative contributions of sedimentation, dolomitization, karstification, and tectonic dissolution, require further investigation. These unresolved issues significantly restrict the prediction of favorable exploration targets in the deep Cambrian succession.

Based on 3D seismic data, drilling information, core observations, thin-section petrography, and reservoir characterization data from the Yudu area, this study systematically investigates the distribution characteristics of Cambrian platform-margin high-energy shoals and the formation mechanisms of high-quality dolomite reservoirs. The objectives of this study are to: characterize the seismic and sedimentological features of platform-margin shoal complexes; clarify the controlling effects of the Yudu rift trough and fault-controlled paleogeomorphology on shoal development; determine the reservoir space types and multi-stage diagenetic evolution of the Cambrian dolomite reservoirs; and establish a genetic model for the development of high-quality reservoirs and hydrocarbon accumulation in the Yudu platform-margin belt. The results provide new insights into the development

mechanisms of deep Cambrian carbonate reservoirs and offer important guidance for further hydrocarbon exploration in the Tarim Basin.

2. Geological Setting

2.1. Regional Tectonic Setting

The Tarim Basin is one of the largest superimposed cratonic basins in China and contains a complete Neoproterozoic–Paleozoic marine carbonate succession with significant hydrocarbon resources [33–35]. Tectonically, the basin is bounded by the Tianshan Orogenic Belt to the north, the Kunlun Orogenic Belt to the south, and the Altun Orogenic Belt to the southeast [36–38]. During the Early Paleozoic, the Tarim Basin evolved as a stable cratonic carbonate platform affected by multiple episodes of intracratonic rifting and extensional tectonism [34,39,40]. These tectonic events controlled the development of paleouplifts, rift troughs, platform-margin slope-break belts, and carbonate facies differentiation, thereby exerting important influences on hydrocarbon generation, reservoir development, and accumulation (Figure 1a,b).

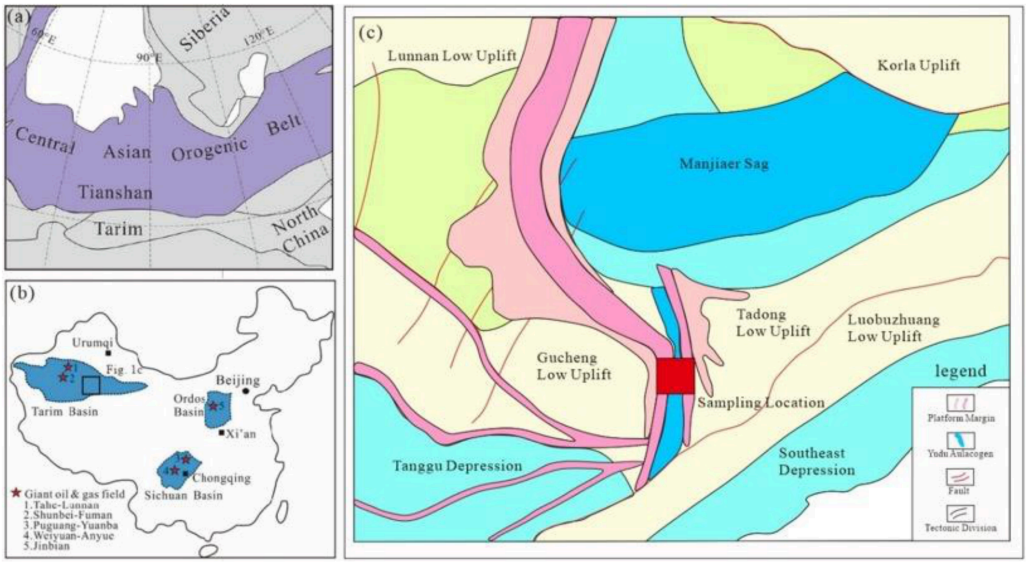


Figure 1. (**a**) Schematic tectonic map of the Central Asian Orogenic Belt, where the purple shaded area delineates the scope of the Central Asian Orogenic Belt. (**b**) Distribution sketch of major giant oil and gas fields across China; the blue polygons mark the primary petroliferous basins in the country. (**c**) Regional geological map of the Yudu area. The red rectangular box denotes the core sampling region; light blue areas correspond to depressions, while pale yellow areas represent paleo-uplifts.

During the Early–Middle Cambrian, regional extensional tectonism resulted in the formation of several intracratonic rift troughs in the Tarim Basin, including the Awati-Manjiaer rift system and associated local rift troughs distributed along the western and central parts of the basin [18]. These rift troughs generally exhibit steep fault-controlled margins and inherited paleogeomorphic relief, providing favorable conditions for the development of platform-margin reef–shoal complexes and source rock deposition [41,42]. Previous exploration results indicate that areas adjacent to Cambrian rift troughs commonly exhibit superior source-reservoir assemblages and favorable hydrocarbon accumulation conditions.

The Yudu area is located in the western slope-break zone of the Tarim Basin and is adjacent to the Yudu rift trough. Structurally, the study area is situated in the transitional zone between the Manxi slope-break belt and the intracratonic rift system [43]. The Cambrian platform margin in this area was strongly controlled by synsedimentary extensional faults and paleogeomorphic slope breaks, resulting in the formation of a fault-controlled

platform-margin depositional system [44,45]. Seismic interpretation reveals that multiple stages of platform-margin migration and progradation occurred during the Cambrian, forming large-scale high-energy shoal complexes distributed along the margin of the Yudu rift trough.

In addition to controlling sedimentary facies differentiation, the Yudu rift trough also played an important role in hydrocarbon generation and migration [46,47]. The proximity of the platform-margin shoal complexes to hydrocarbon kitchens provided favorable conditions for "intra-source accumulation" within the Cambrian succession [48–50]. Drilling data from nearby exploration wells indicate high-pressure coefficients, abundant hydrocarbon shows, and large gas-column heights in platform-margin reservoirs close to the source rock depocenters, suggesting efficient hydrocarbon charging and preservation conditions in the study area (Figure 1c).

2.2. Stratigraphic Framework

The Cambrian succession in the Yudu area mainly consists of a thick carbonate-dominated sedimentary system deposited on a carbonate platform margin. From bottom to top, the Cambrian strata include the Yurtus Formation, Xiaoerbulake Formation, Wusonggeer Formation, and overlying Middle–Upper Cambrian carbonate units [6,51,52]. The lower Cambrian succession is characterized by mixed siliciclastic-carbonate deposits and organic-rich source rocks, whereas the Middle–Upper Cambrian succession is dominated by platform carbonates, dolomites, microbial buildups, and shoal complexes [53,54].

The Yurtus Formation mainly consists of dark mudstone and argillaceous carbonate rocks deposited in a deep-water shelf to slope environment and represents one of the most important hydrocarbon source rock intervals in the Tarim Basin [20,55,56]. Overlying the Yurtus Formation, the Xiaoerbulake and Wusonggeer Formations are dominated by shallow-water platform carbonates and dolomites deposited under relatively high-energy conditions [8,57,58]. During the Middle–Late Cambrian, continuous platform-margin progradation and shoal development occurred along the slope-break belt adjacent to the Yudu rift trough, forming thick accumulations of granular dolomites, microbial dolomites, and reef–shoal complexes [59].

The Cambrian carbonate succession is widely distributed across the Tarim Basin and constitutes an important deep to ultra-deep marine carbonate system. Its present burial depth varies substantially across the basin as a result of differential subsidence, uplift, erosion, and subsequent tectonic reworking. In the Yudu–Gucheng region, the Cambrian succession occurs at considerable burial depths, with drilling and core data documenting Cambrian carbonate reservoirs at approximately a 6.7–7.4 km depth in several wells, including observations at 6735–7373 m in the Gucheng and Yudu exploration areas. Deeper drilling data from the Yudu exploration domain further document Cambrian-related intervals at an approximately 8.3–8.7 km depth, highlighting the ultra-deep nature of the target succession. The carbonate-dominated succession is characterized by substantial vertical thickness and strong lateral facies variability, with shallow-platform, platform-margin shoal, slope, and rift-trough deposits developed across the basin. Within the Yudu–Gucheng platform-margin belt, reservoir-bearing intervals are concentrated in the Cambrian platform-margin shoal complexes; individual effective reservoir intervals range from approximately 67.4 to 268 m in representative wells, demonstrating the considerable vertical development of reservoir-prone carbonate bodies within the deeply buried succession. These characteristics make the Yudu area a representative setting for investigating the development and preservation of Cambrian platform-margin reservoirs under ultra-deep burial conditions.

Sequence stratigraphic analysis indicates that multiple third-order depositional cycles developed within the Cambrian succession. The stratigraphic framework is characterized by repeated upward-shallowing carbonate cycles controlled by relative sea-level fluctuations and synsedimentary tectonic activity [60–62]. Several sequence boundaries and flooding surfaces can be identified in seismic and drilling data, reflecting episodic platform-margin migration and facies reorganization during the Cambrian evolution.

In this study, carbonate rock samples spanning the upper Cambrian and lower Ordovician strata were collected from the Yudu area for petrographic and reservoir analysis (Figure 2).

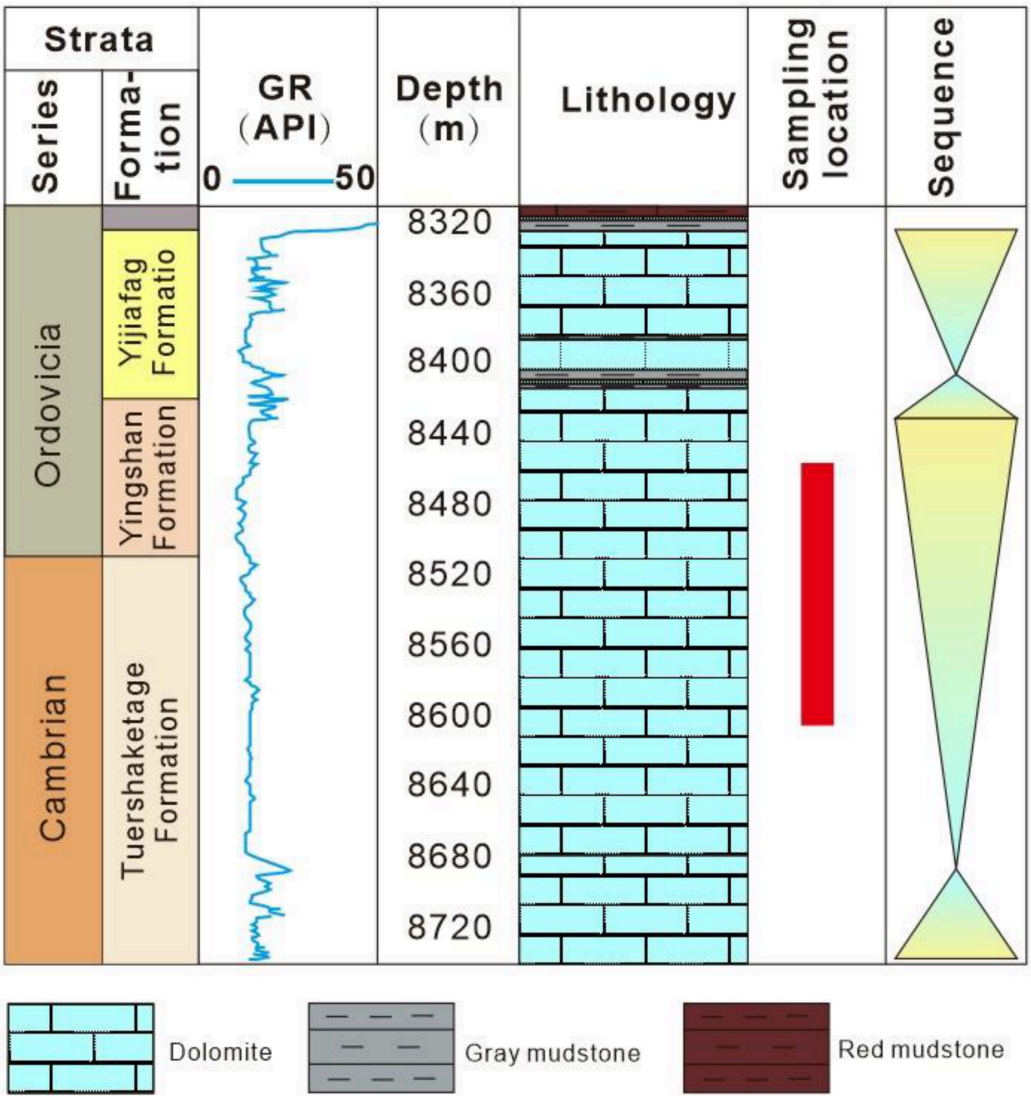


Figure 2. Stratigraphic column of the Yudu area. GR (gamma ray) denotes the gamma-ray log response, and API refers to American Petroleum Institute units, the standard unit used to report gamma-ray log values. The stratigraphic sequences illustrate vertical grain-size trends from relatively coarse-grained to finer-grained deposits, with grain size decreasing progressively from coarse- to fine-grained lithologies.

2.3. Cambrian Platform-Margin Evolution

The Cambrian platform margin in the Yudu area experienced multi-stage evolution controlled by synsedimentary fault activity and relative sea-level fluctuations [63]. During the early stage of platform development, extensional tectonism generated pronounced paleogeomorphic relief along the margin of the Yudu rift trough, leading to the

formation of steep slope-break belts and localized paleohighs [21,25]. These geomorphic conditions promoted the accumulation of high-energy shoal deposits along the platform margin [14,42,64].

As carbonate production increased during the Middle Cambrian, the platform margin progressively prograded toward the rift trough, resulting in the vertical superposition and lateral migration of multiple shoal complexes [65–67]. Seismic profiles reveal characteristic progradational reflection patterns and mound-shaped external geometries associated with the platform-margin shoals. Several stages of shoal development can be recognized within the Cambrian succession, indicating repeated sedimentary aggradation and margin advancement.

The inherited paleogeomorphic framework also controlled the distribution of subsequent diagenetic modifications and reservoir development [68–70]. Platform-margin shoals composed of granular carbonates and microbial dolomites provided favorable material foundations for reservoir formation. Later dolomitization, karstification, and tectonic dissolution further enhanced the reservoir quality by generating abundant intercrystalline pores, moldic pores, dissolution vugs, and fracture–cavity systems [71,72]. Consequently, the Cambrian platform-margin belt in the Yudu area evolved into a favorable exploration target characterized by the superposition of sedimentary, diagenetic, and hydrocarbon accumulation advantages.

3. Materials and Methods

3.1. Seismic Data and Interpretation

Drilling and wireline logging data from representative exploration wells in the Yudu–Gucheng area were integrated with the seismic interpretation. The well dataset included conventional wireline logs, drilling records, mud-logging information, hydrocarbon shows, and available reservoir-test data. Gamma-ray, resistivity, density, neutron, and sonic responses, where available, were examined together with lithological descriptions to identify stratigraphic contacts and lithofacies variations.

Well–seismic calibration was performed using the stratigraphic markers identified from the drilling and logging data. These markers were used to constrain the interpretation of the Cambrian top and base, major internal stratigraphic interfaces, and sequence boundaries in the seismic volume. Reservoir intervals were identified by integrating lithological characteristics, logging responses, drilling behavior, gas shows, and available reservoir-test results rather than relying on a single logging criterion.

Reservoir characteristics were compiled from available core analyses and well-log interpretations, including effective reservoir thickness, porosity, reservoir type, and hydrocarbon-bearing characteristics. Particular attention was paid to intervals characterized by fracture–vuggy and pore–vuggy dolomite reservoirs, as these represent the principal reservoir types recognized in the study area. Drilling losses, overflow, elevated gas contents, and abnormal pressure coefficients were recorded as supporting evidence for hydrocarbon-bearing intervals where these observations were available.

3.2. Drilling, Logging, and Reservoir Test Data

Drilling data from several exploration wells in the Yudu area were systematically analyzed in this study. The datasets include conventional logging curves, drilling records, reservoir test results, mud logging information, and hydrocarbon show data. Reservoir intervals within the Cambrian platform-margin succession were identified through integrated interpretation of lithology, porosity response, gas shows, and drilling fluid anomalies.

Reservoir physical properties, including porosity, reservoir thickness, and reservoir types, were compiled from core analyses and logging interpretations. The studied reser-

voirs mainly occur in the Qiulitage and Awatage Formations and are characterized by fracture–vuggy and pore–vuggy dolomite reservoirs with variable reservoir quality. Several wells encountered thick reservoir intervals and abundant hydrocarbon shows, indicating favorable exploration potential in the platform-margin shoal belts.

Drilling and testing data also provide important evidence for hydrocarbon accumulation conditions in the study area. Overflow phenomena, drilling losses, high gas contents, and abnormal pressure coefficients were observed in multiple wells, suggesting effective hydrocarbon charging and preservation within the Cambrian reservoirs.

3.3. Core Observation and Petrographic Analysis

Representative Cambrian core intervals from key exploration wells were examined to characterize lithology, sedimentary structures, pore types, fractures, dissolution features, and hydrocarbon occurrence. Core descriptions were integrated with corresponding well-log and stratigraphic information to establish lithofacies and reservoir correlations.

Thin-section petrographic observations were conducted using conventional transmitted-light microscopy. The analysis focused on carbonate grain types, depositional textures, microbial and algal fabrics, dolomite crystal textures, pore types, fracture characteristics, and diagenetic relationships. The principal lithofacies examined include granular dolomite, microbial dolomite, oolitic dolomite, brecciated dolomite, and fine- to medium-crystalline dolomite. Pore systems were classified into intercrystalline pores, intergranular dissolution pores, moldic pores, intragranular dissolution pores, fracture-related dissolution pores, and vuggy or karst-related cavities [73–75].

Diagenetic relationships were evaluated from cross-cutting relationships, replacement textures, dissolution boundaries, and pore-filling relationships observed in the cores and thin sections. These observations were used to distinguish major stages of dolomitization, dissolution, burial modification, and tectonic fracturing. Interpretations of diagenetic processes were compared with previously established carbonate diagenetic models [76–79].

3.4. Sedimentary Facies and Reservoir Characterization

Sedimentary facies were interpreted by integrating lithologic assemblages, vertical facies successions, core sedimentary structures, well-log responses, seismic reflection configurations, and external geometries of carbonate bodies. Platform-margin shoals were identified based on the combined occurrence of grain-rich and microbial carbonate lithofacies, upward-shallowing successions, mound-shaped or prograding seismic geometries, and their spatial relationship to the platform-margin slope break.

Reservoirs were characterized by integrating lithofacies, pore systems, fracture characteristics, dissolution features, and available physical-property data. Reservoir types were classified according to their dominant reservoir-space assemblages, including pore–vuggy, fracture–vuggy, and related composite types. Reservoir distribution was then compared with the interpreted platform-margin shoal architecture and major fault systems.

Finally, the integrated seismic, well, core, petrographic, and reservoir datasets were used to construct a geological model linking fault-controlled paleogeomorphology, platform-margin shoal development, dolomitization, dissolution, fracture development, and hydrocarbon occurrence. Importantly, the genetic interpretations presented in the Section 6 were restricted to relationships supported by the integrated observational datasets.

All geological, well, core, and reservoir datasets analyzed in this study were obtained from the exploration and research data available for the Yudu–Gucheng area. Because the seismic and drilling datasets are derived from an industry exploration program, detailed

acquisition specifications and proprietary processing parameters are not publicly available and are therefore not reported where they cannot be independently verified.

4. Characteristics of Platform-Margin High-Energy Shoals

4.1. Seismic Reflection Characteristics of Platform-Margin Shoals

The Cambrian platform-margin shoals in the Yudu area exhibit distinctive seismic reflection characteristics that can be clearly identified on 3D seismic profiles. The shoal complexes are mainly distributed along the slope-break belt adjacent to the Yudu rift trough and display mound-shaped to lenticular external geometries with medium- to strong-amplitude reflections. On seismic sections, the platform margin is characterized by obvious progradational reflection configurations, reflecting repeated margin advancement toward the rift trough during the Cambrian.

The seismic reflections within the shoal complexes commonly exhibit chaotic to sub-parallel internal reflection patterns, whereas the platform-margin boundaries are marked by discontinuous oblique reflections and localized downlap terminations (Figure 3). Several seismic sections reveal stacked progradational units with repeated lateral migration of shoal bodies, indicating multistage development of the platform-margin system. The mound-shaped external geometries and prograding reflection patterns are interpreted as seismic responses of high-energy carbonate shoal complexes developed along the platform margin.

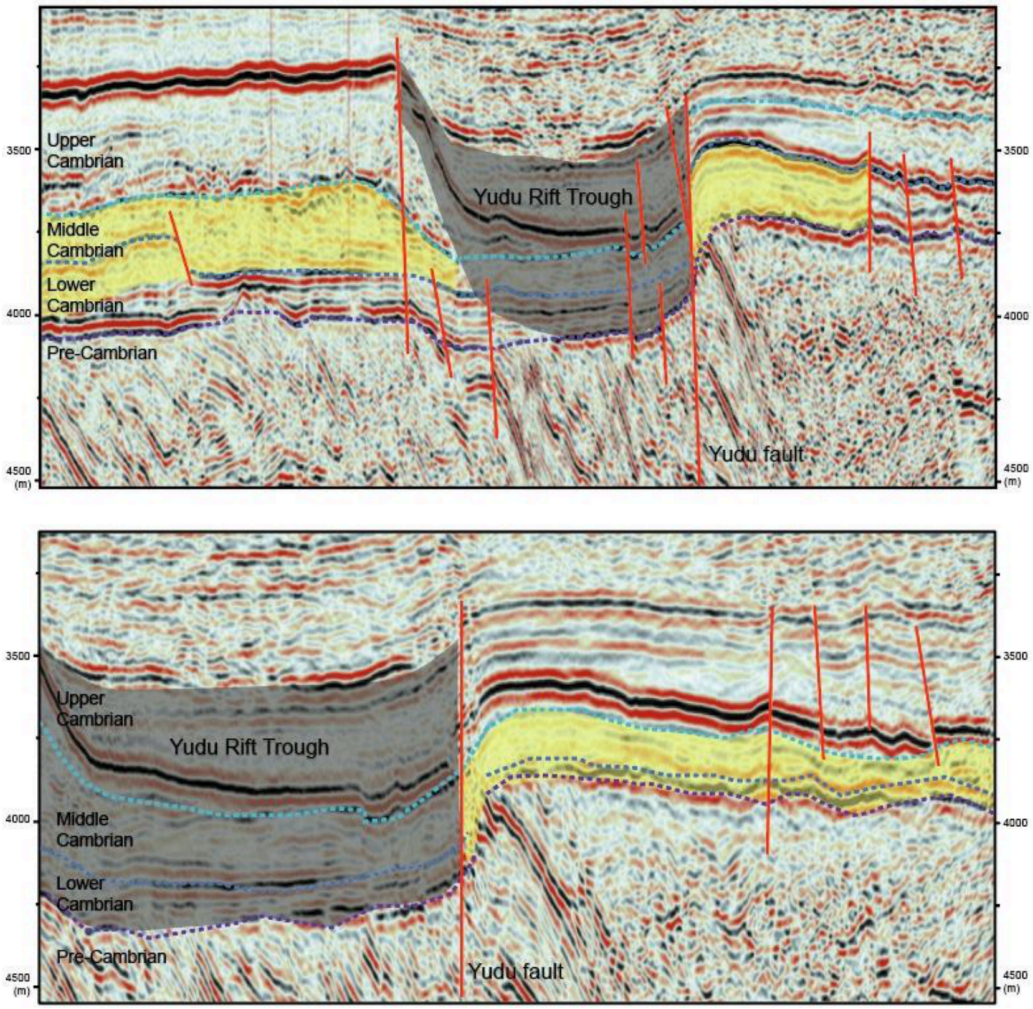


Figure 3. Seismic architecture of the Yudu area. The yellow shaded interval denotes the Early–Middle Cambrian progradational platform-margin mound–shoal complex. Red lines represent major faults.

NS-oriented seismic profile provides an independent view of the structural and stratigraphic architecture of the Cambrian carbonate succession and complements the original WE-oriented profile (Figure 3). In the NS direction, the Cambrian succession can be traced continuously across the platform-margin zone, while the seismic reflections show systematic changes in dip, continuity, and configuration toward the rift-trough side. The platform-margin interval is characterized by a distinct transition from relatively continuous and subparallel reflections within the platform interior to more inclined and locally discontinuous reflections near the margin. This transition defines the structural and depositional slope-break zone and provides an additional seismic constraint on the location of the platform margin. The NS profile also confirms that the carbonate succession is structurally segmented by major faults, with localized changes in reflector geometry and thickness adjacent to fault zones. The agreement between the WE- and NS-oriented profiles indicates that the platform-margin architecture is not restricted to a single seismic section but represents a spatially coherent structural–stratigraphic feature within the 3D seismic volume.

The top and bottom boundaries of the Cambrian succession, the top Middle Cambrian interface, and the limestone top interface can be continuously traced across the study area, providing important stratigraphic constraints for identifying the distribution of the shoal complexes. Synsedimentary faults associated with the Yudu rift trough locally disrupted the continuity of seismic reflections and controlled the morphology of the platform-margin slope-break zone. The close spatial relationship between fault activity and platform-margin shoal distribution indicates strong tectono-sedimentary coupling during the Cambrian evolution.

4.2. Spatial Distribution and Evolution of Shoal Complexes

The Cambrian platform-margin shoals in the Yudu area are mainly distributed along the margin of the Yudu rift trough and the western slope-break belt. Seismic interpretation demonstrates that the shoal complexes exhibit obvious lateral continuity and vertical superposition, forming large-scale platform-margin sedimentary bodies extending along the strike of the slope-break zone.

The NS-oriented seismic profile further constrains the lateral distribution and stratigraphic organization of the platform-margin shoal complexes (Figure 3). Along this direction, the mound-shaped to prograding seismic bodies occur within a relatively restricted stratigraphic interval and show clear vertical stacking, whereas their lateral continuity decreases toward the adjacent deeper-water domain. The transition from relatively flat-lying platform reflections to inclined and prograding reflections provides evidence for the spatial migration of the platform margin through time. In combination with the WE-oriented profile, the two intersecting seismic sections demonstrate that the shoal complexes form three-dimensional carbonate buildup bodies rather than isolated features confined to individual profiles. Their repeated vertical superposition and basinward changes in seismic geometry indicate successive phases of platform-margin development and migration during Cambrian deposition. This cross-directional seismic evidence provides a more robust basis for delineating the stratigraphic distribution and three-dimensional architecture of the platform-margin shoal system.

Multiple stages of shoal development can be recognized in the Cambrian succession. The earlier shoal bodies generally developed near the initial slope-break zone controlled by synsedimentary faults, whereas later shoals progressively migrated basinward due to continuous platform progradation. This evolutionary pattern produced vertically stacked shoal complexes characterized by repeated aggradation and progradation. Several seismic sections reveal clear evidence of margin advancement toward the rift trough, indicating sustained carbonate productivity under relatively high-energy depositional conditions.

In the Gucheng area, at least four stages of platform-margin shoal development can be identified within the Cambrian succession. The superposition of multistage shoals resulted in the formation of thick carbonate buildup complexes with favorable reservoir development potential. Seismic and drilling data further indicate that the distribution of high-quality reservoirs is closely related to the spatial distribution of these multistage shoal complexes.

The platform-margin shoals also exhibit significant facies differentiation from the platform interior toward the rift trough. The platform interior is dominated by relatively low-energy dolomitic deposits, whereas the platform-margin zone is characterized by granular shoals, microbial buildups, and local collapse-related deposits. The slope area adjacent to the rift trough locally contains gravity-flow deposits and collapse breccias associated with margin instability and synsedimentary fault activity.

4.3. Sedimentary Characteristics of High-Energy Shoals

Core observations and thin-section analyses indicate that the Cambrian platform-margin shoals in the Yudu area were deposited under high-energy hydrodynamic conditions (Figure 4a–c). The dominant lithologies include granular dolomite, microbial dolomite, oolitic dolomite, algae-bearing dolomite, and bioclastic dolomite. These lithologies commonly contain grain-supported fabrics and locally preserve residual granular textures, indicating deposition in shallow-water, high-energy carbonate shoal environments.

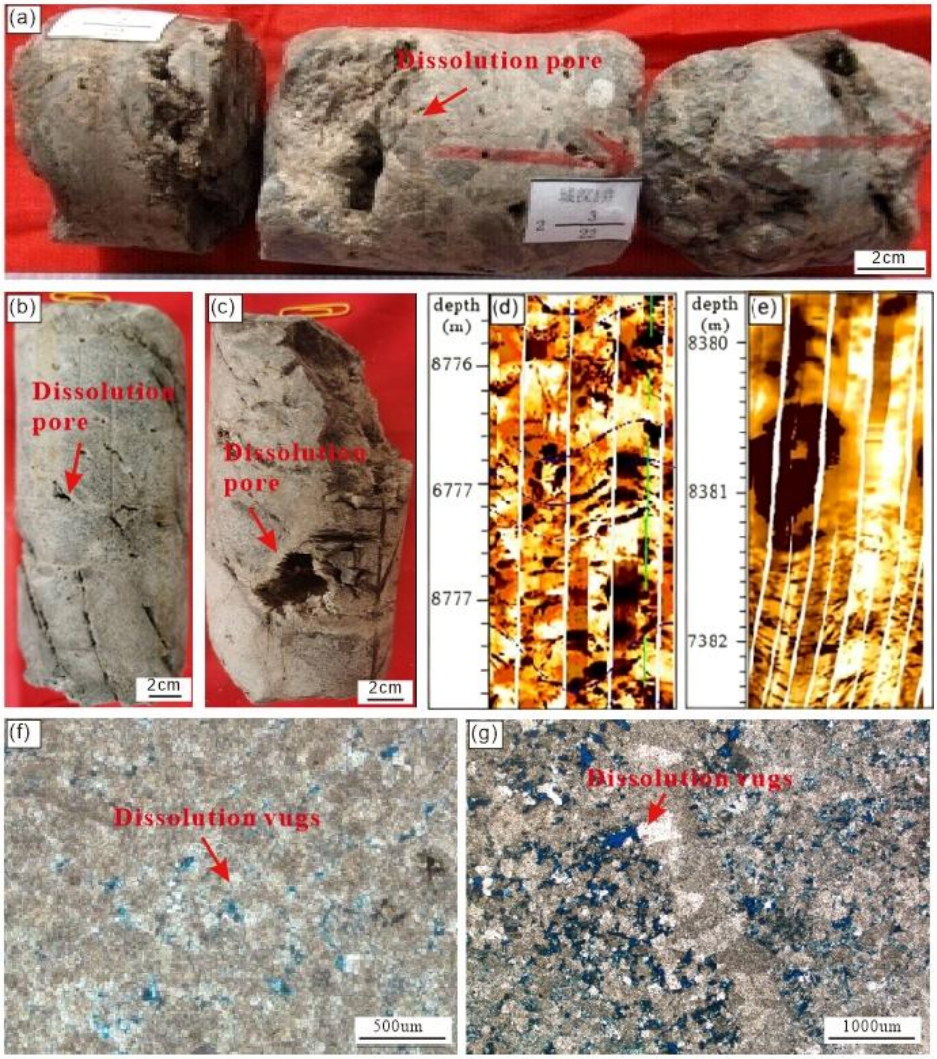


Figure 4. (**a**–**c**) Core photographs, (**d**,**e**) imaging logging images, and (**f**,**g**) petrographic images from the Yudu area.

Microbial and algal components are widely developed within the shoal complexes. Algal-skeletal grains, microbial framework structures, and grain-supported fabrics are commonly observed in thin sections, suggesting that microbial carbonate production played an important role in the development of the platform-margin shoals. Oolitic and bioclastic grains are locally abundant, further indicating strong hydrodynamic conditions along the platform margin.

Collapse breccias and brecciated dolomites are also locally developed within the shoal complexes and are interpreted to be associated with synsedimentary collapse and later karst-related dissolution processes. The occurrence of collapse-related deposits near the platform margin suggests that tectonic activity and paleogeomorphic relief significantly influenced sedimentary processes and subsequent reservoir modification.

Vertical facies successions observed in drilling cores indicate repeated shallowing–upward depositional cycles within the shoal complexes. Individual cycles commonly begin with relatively low-energy fine-crystalline dolomites and upward transition into granular shoal deposits characterized by algae-bearing and grain-supported fabrics. These vertical facies patterns reflect repeated fluctuations in relative sea level and the repeated establishment of high-energy shoal environments along the platform margin.

4.4. Fault-Controlled Development of Platform-Margin Shoals

The development and distribution of the Cambrian platform-margin shoals in the Yudu area were strongly controlled by synsedimentary fault activity associated with the Yudu rift trough. Seismic interpretation reveals that the platform-margin slope-break belt closely follows the distribution of major basement-involved faults, indicating that tectonic paleogeomorphology exerted a first-order control on carbonate sedimentation.

Synsedimentary faults created steep paleogeomorphic relief and localized high-energy depositional zones along the platform margin. These slope-break belts promoted wave and current reworking, thereby facilitating the accumulation of granular shoal deposits and microbial buildups. Continuous fault activity also controlled accommodation space variations and margin migration during the Cambrian evolution, resulting in the repeated development of shoal complexes along structurally inherited paleohighs.

The close coupling between fault systems and shoal distribution further influenced subsequent reservoir development. Platform-margin shoals located adjacent to major faults commonly experienced stronger dolomitization, dissolution, and fracture modification due to enhanced fluid circulation along tectonic conduits. Consequently, the fault-controlled platform-margin shoals became the most favorable zones for the development of high-quality dolomite reservoirs in the Yudu area.

Overall, the Cambrian platform-margin system in the Yudu area represents a typical fault-controlled carbonate platform margin characterized by multistage progradational shoal development, strong tectono-sedimentary coupling, and favorable conditions for subsequent reservoir enhancement.

5. Characteristics of Cambrian Dolomite Reservoirs

5.1. Reservoir Lithology and Petrological Characteristics

The Cambrian reservoirs in the Yudu area are dominated by dolomite reservoirs developed within platform-margin high-energy shoal complexes (Figure 5). Core observations and thin-section analyses indicate that the reservoir lithologies mainly include fine- to medium-crystalline dolomite, granular dolomite, algae-bearing dolomite, microbial dolomite, oolitic dolomite, and locally brecciated dolomite.

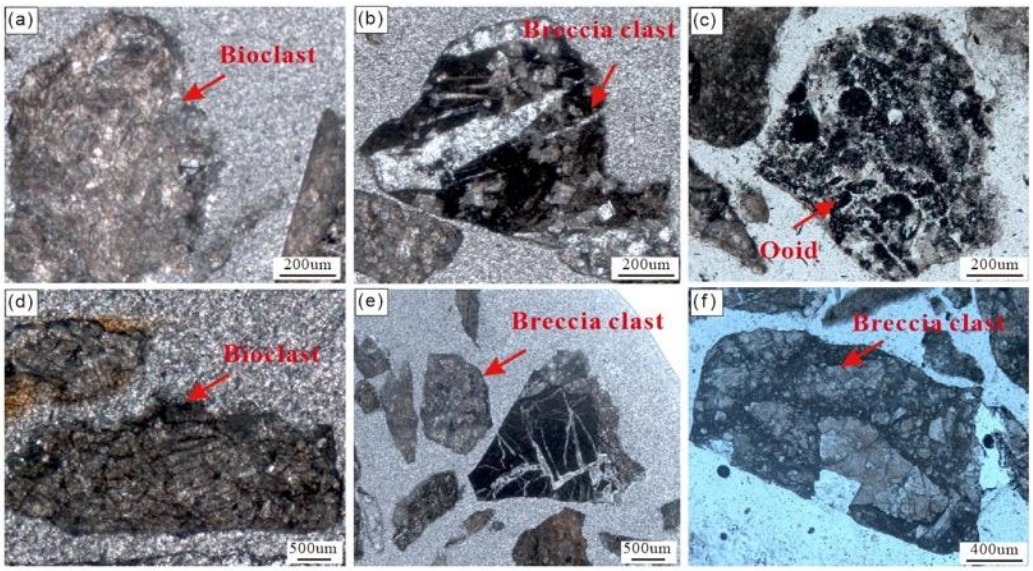


Figure 5. Petrographic micrographs of dolomite and breccia samples collected from the Yudu area. (**a**) Bioclastic dolomite; (**b**) residual oolitic dolomite; (**c**) tectonic karst breccia; (**d**) bioclastic dolomite; (**e**) tectonic karst breccia; (**f**) tectonic karst breccia.

Granular dolomites are the most important reservoir lithofacies and are widely distributed within the platform-margin shoal bodies. Granular textures are commonly preserved despite pervasive dolomitization, including algal fragments, bioclastic grains, and oolitic structures. Grain-supported fabrics and locally preserved framework textures indicate deposition under strong hydrodynamic conditions in shallow-water high-energy shoal environments.

Microbial dolomites are also extensively developed within the shoal complexes and commonly contain microbial framework fabrics, stromatolitic textures, and algae-related structures. The microbial framework provided favorable primary pore frameworks and enhanced resistance to compaction during burial. In several wells, microbial dolomites exhibit strong dissolution modification and locally develop abundant vuggy pores and fracture-related dissolution systems.

Brecciated dolomites and collapse-related lithologies occur locally within the platform-margin reservoirs. These breccias are characterized by irregular clast-supported fabrics and dissolution-related matrix filling, indicating strong karstification and collapse modification during the post-depositional evolution of the carbonate platform margin.

Petrographic observations further reveal widespread recrystallization and dolomitization in the Cambrian carbonate succession. Most reservoirs are dominated by fine- to medium-crystalline dolomite with locally developed coarse-crystalline dolomite. The degree of recrystallization varies significantly among different shoal intervals, reflecting complex diagenetic modification histories associated with burial fluids, tectonic activity, and dissolution processes.

5.2. Reservoir Space Types and Pore System Characteristics

The Cambrian dolomite reservoirs in the Yudu area are characterized by complex pore–fracture systems formed through multistage diagenetic modification. The main reservoir space types include intercrystalline pores, intergranular dissolution pores, moldic pores, intragranular dissolution pores, dissolution vugs, fractures, and fracture–cavity systems (Figure 6).

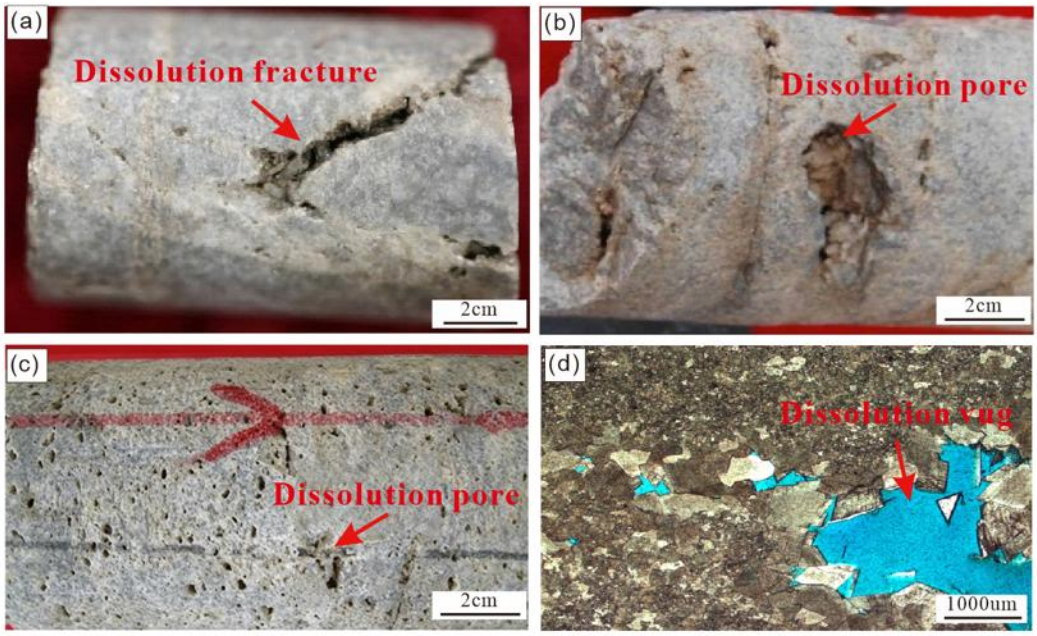


Figure 6. Core photographs and micrographs showing dissolution pore–fracture development in dolomite samples from the Yudu area. (**a**) Medium-crystalline dolomite with well-developed dissolution pores and fractures; (**b**) coarse-crystalline dolomite with abundant dissolution pores; (**c**) fine-to-medium crystalline dolomite with widespread dissolution pores; (**d**) micrograph of dolomite showing well-developed dissolution vugs.

Intercrystalline pores are widely developed in fine- to medium-crystalline dolomites and constitute one of the most common reservoir space types. These pores are mainly related to dolomitization-induced crystal reorganization and partial preservation of primary pore systems. In granular dolomites, intergranular dissolution pores and moldic pores are particularly well-developed due to the selective dissolution of unstable carbonate grains and early pore enhancement.

Thin-section observations indicate that many dissolution pores exhibit strong fabric selectivity. Grain-supported shoal deposits commonly contain preferentially dissolved algal grains, bioclastic fragments, and oolitic particles, forming irregular moldic and intragranular pores. In several samples, dissolution pores are interconnected by fractures, resulting in the formation of effective pore–fracture networks that significantly improve reservoir connectivity.

Fractures are extensively developed within the Cambrian reservoirs and include tectonic fractures, dissolution-enlarged fractures, and fracture-associated vugs. Some fractures are partially filled with bitumen or late-stage calcite, whereas others remain unfilled and serve as effective hydrocarbon migration pathways and storage spaces. Core observations reveal that fracture-related dissolution is especially strong near major fault zones and unconformity surfaces.

Large dissolution cavities and fracture–cavity systems are locally developed within the platform-margin reservoirs. These cavities commonly occur along fractures, bedding interfaces, and karst-related dissolution zones, suggesting strong structural and fluid-control effects during reservoir evolution. In some intervals, dissolution cavities exceed several meters in vertical scale and are associated with severe drilling losses and hydrocarbon shows during drilling operations.

5.3. Physical Properties and Reservoir Distribution

The Cambrian reservoirs in the Yudu area generally exhibit low matrix porosity but locally develop relatively high-quality pore–fracture–vug systems due to multistage dissolution and tectonic modification. Reservoir porosity is highly heterogeneous and varies significantly among different lithofacies and structural positions.

According to core and logging interpretation data, the effective reservoir intervals are mainly concentrated within the platform-margin shoal complexes of the Cambrian. Reservoir thicknesses commonly range from tens of meters to more than 200 m in favorable shoal development zones. For example, a new drilled well encountered approximately 67.4 m of effective reservoir with porosity values ranging from 1.8% to 11.2%, whereas another well drilled in 2024 encountered up to 268 m of reservoir intervals in the Awatage Formation.

Reservoir quality is closely related to sedimentary facies and tectonic position (Figure 7). High-quality reservoirs are preferentially developed in platform-margin shoal bodies adjacent to the Yudu rift trough and major fault systems. These reservoirs commonly exhibit enhanced dissolution, better fracture development, and stronger fluid modification compared with relatively low-energy intraplatform deposits.

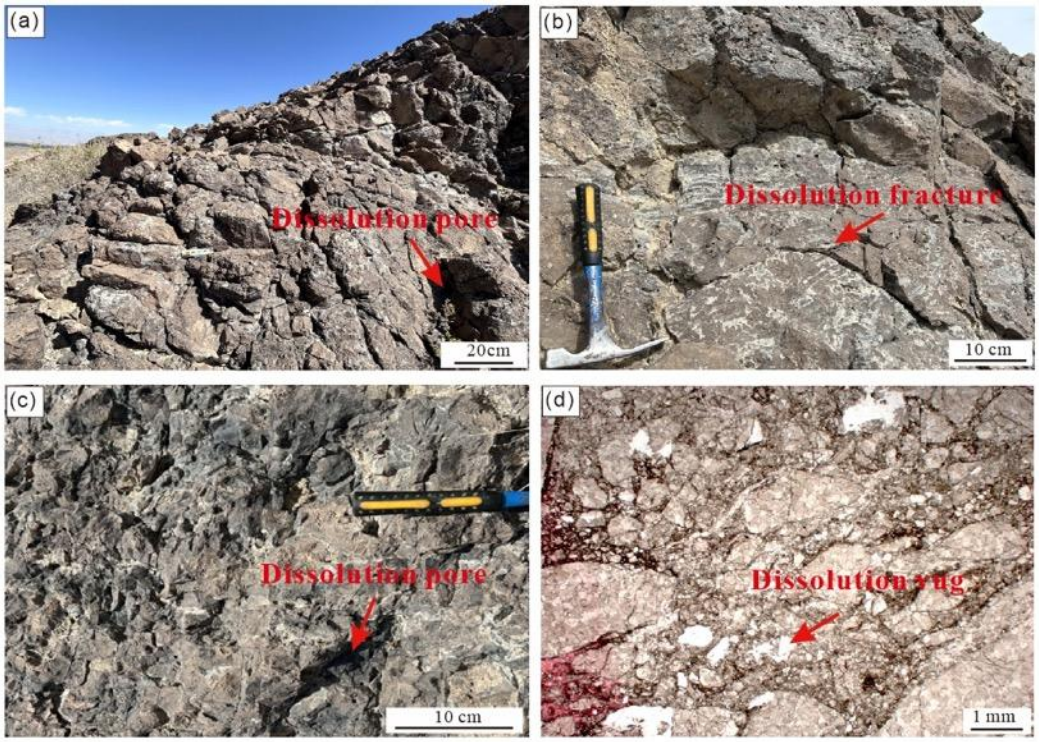


Figure 7. (**a**–**c**) Field outcrop photos and (**d**) thin-section micrographs of reservoir rocks from the Yudu area. (**a**) Fault-controlled mound-shoal complexes with well-developed fractures and pores; (**b**) stratiform dissolution pores and fractures developed within fault-triggered collapse breccia bodies; (**c**) collapse breccia bodies abundant in dissolution pores; (**d**) irregular dissolution vugs and intergranular dissolution vugs are visible, with intergranular vugs distributed along tectonic dissolution fractures.

Based on reservoir space assemblages and physical property characteristics, the Cambrian reservoirs in the Yudu area can be classified into three major reservoir types: (1) fracture–vuggy reservoirs; (2) pore–vuggy reservoirs; (3) fracture–cavity reservoirs. Among these, fracture–vuggy dolomite reservoirs represent the dominant reservoir type within the platform-margin shoal complexes. The combination of dissolution pores, tectonic fractures, and karst cavities significantly improves storage capacity and permeability under ultra-deep burial conditions.

6. Discussion

6.1. Fault-Controlled Paleogeomorphology and Development of Platform-Margin Shoals

The distribution and architecture of Cambrian platform-margin high-energy shoals in the Yudu area are closely associated with the inherited structural framework of the Yudu rift trough [80]. The seismic results show that the platform margin developed preferentially along a persistent slope-break belt adjacent to the rift trough, rather than being distributed uniformly across the carbonate platform (Figure 3). Major faults occur along or near this slope break, and changes in reflector geometry and stratigraphic thickness are commonly observed across the fault zones. The seismic profiles provide consistent evidence for this relationship from two directions, showing that the margin-related carbonate bodies are spatially associated with a three-dimensional structural boundary rather than representing isolated features on a single seismic section. This geometry indicates that the initial platform morphology was strongly influenced by inherited fault-controlled relief. Similar relationships between intracratonic extension, fault-bounded topography, and carbonate platform-margin development have been documented in other rift-related carbonate systems, where synsedimentary structures created persistent accommodation contrasts and influenced the position of carbonate factories [81–83].

The structural framework favored the concentration of high-energy carbonate deposits along the platform margin. Extensional faulting generated relief between shallow platform areas and the adjacent rift depression, establishing a narrow slope-break zone where carbonate production and sediment redistribution were enhanced. The occurrence of granular and microbial carbonate facies within these bodies is consistent with shallow, high-energy deposition [15,84,85]. Similar relationships between synsedimentary faulting, structural relief, and carbonate accumulation have been documented in other Paleozoic carbonate platforms [86–88].

The platform margin was not stationary through time. Progradational reflection configurations, lateral shifts of mound-shaped seismic bodies, and vertically superimposed shoal intervals indicate repeated changes in the position of the depositional margin. These features are particularly important because they distinguish the Yudu system from a simple, fixed platform rim. The observed migration can be related to changes in the balance among tectonic subsidence, accommodation creation, carbonate production, sediment supply, and relative sea level. During periods when tectonic subsidence increased accommodation in the riftward direction, carbonate accumulation could progressively extend toward the basin. Conversely, when carbonate production exceeded accommodation creation, the margin could aggrade or prograde across the available accommodation. Thus, the observed seismic stacking patterns are better interpreted as the sedimentary response to changing accommodation conditions than as evidence for continuous fault activity alone. This interpretation is consistent with carbonate-platform models in which synsedimentary tectonism modifies accommodation and thereby affects the position and geometry of facies belts [89–91].

The four-stage evolutionary framework shown in Figure 8 provides a broader context for this relationship. During the Middle–Lower Cambrian extensional stage, the development of the Yudu rift trough established the initial slope-break framework and separated shallow platform areas from relatively deep depressions [92–94]. During the subsequent Upper Cambrian stage, relatively balanced sedimentation allowed carbonate bodies to aggrade and expand across the structurally favorable platform margin. Renewed extensional activity during the Early–Middle Ordovician further modified the inherited relief and promoted another phase of basinward progradation [95–97]. Although the later Ordovician evolution extends beyond the main Cambrian depositional interval considered here, it is relevant because it demonstrates the persistence of the inherited structural framework. In

this sense, the importance of fault-controlled paleogeomorphology lies not simply in its role during the initial formation of the platform margin, but also in its capacity to guide subsequent sediment accumulation along a repeatedly reactivated structural trend. The geological history supports a model of long-lived structural inheritance rather than the independent formation of individual shoal bodies (Figure 8).

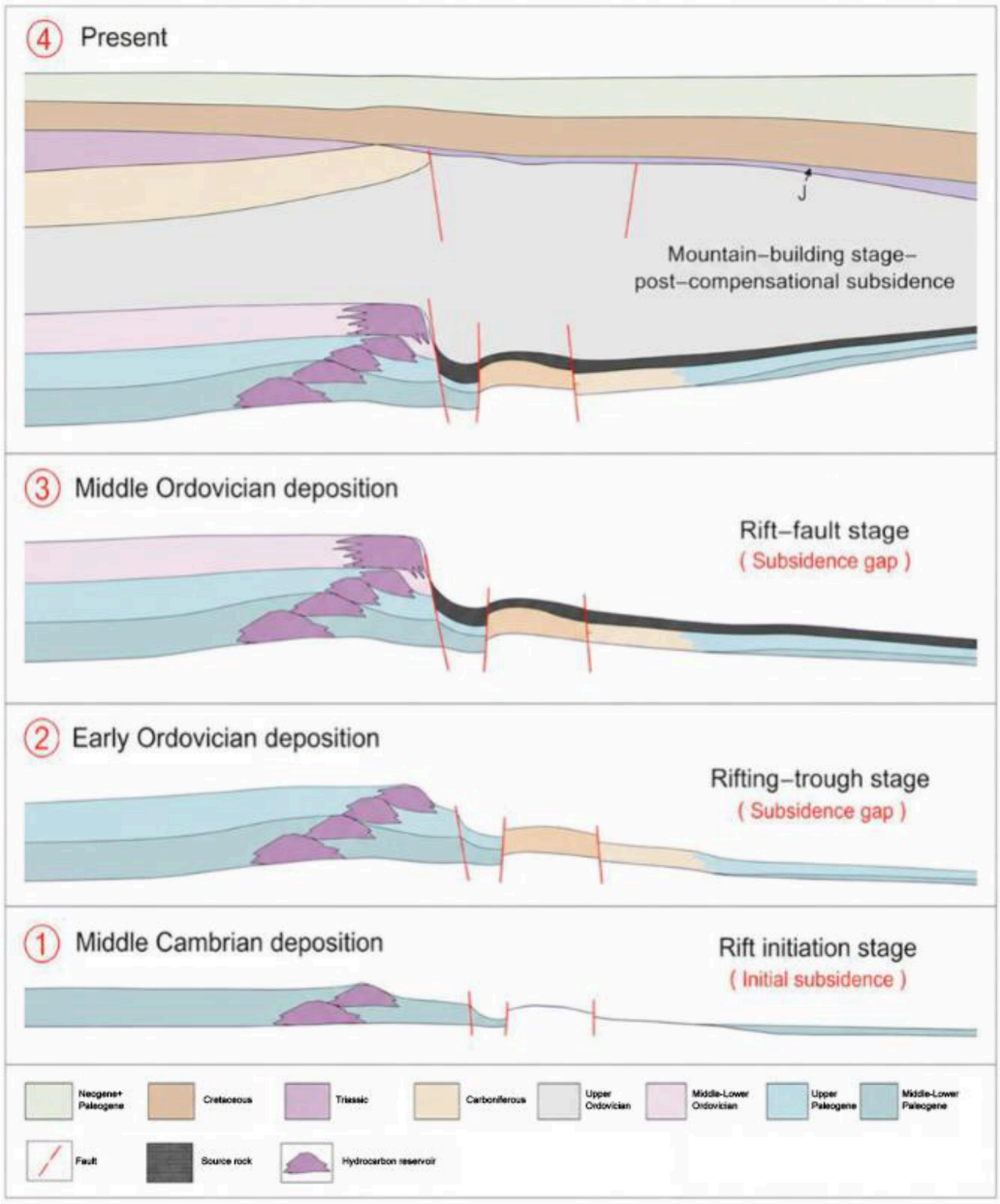


Figure 8. Schematic diagram of tectonic evolution in the Yudu area.

This structural inheritance has implications for the distribution of reservoir-prone intervals. Shoal complexes repeatedly developed near the same slope-break and paleohigh belts, allowing successive depositional bodies to be vertically stacked or laterally superimposed [15,98,99]. The resulting stratigraphic architecture is important because the reservoir intervals are not randomly distributed within the Cambrian succession; instead, thicker reservoir-bearing intervals tend to occur where multiple phases of shoal development overlap. The relationship between shoal stacking and reservoir development is also supported by drilling data, which show that effective reservoirs are concentrated in platform-margin shoal intervals rather than being evenly distributed through the carbonate succession.

However, the structural position and depositional facies alone cannot account for the final reservoir quality. The favorable primary fabric of the shoals provided the initial pore framework, whereas subsequent early dolomitization helped stabilize and reorganize this framework during burial. Later dissolution and fracture development further modified and connected the preserved pore system, producing the observed pore–fracture–vug assemblages. The significance of fault-controlled paleogeomorphology is therefore primarily that it established and repeatedly preserved the depositional setting in which reservoir-prone carbonate facies could develop.

Synsedimentary faulting established the paleogeomorphic template, whereas variations in accommodation and carbonate production controlled subsequent shoal growth, migration, and stacking [100–102]. The resulting architecture records long-term tectono-sedimentary inheritance: faults influenced the position of the slope break, the slope break focused carbonate accumulation, and repeated shoal development produced vertically and laterally extensive reservoir-prone intervals [103–105]. This interpretation provides a geological basis for linking the structural evolution of the Yudu rift trough to the later diagenetic and reservoir-forming processes discussed below, but does not imply that faulting alone generated the present reservoir properties.

6.2. Sedimentary–Diagenetic Coupling and Preservation of Primary Reservoirs

The preservation of effective reservoir space at ultra-depth requires an initial carbonate framework capable of resisting prolonged compaction and cementation [106–108]. In the Yudu area, the distribution of effective reservoirs is closely associated with platform-margin high-energy shoals, where granular, microbial, algal-bearing, and oolitic dolomites constitute the principal reservoir lithofacies. The core and petrographic observations show that these rocks commonly retain grain-supported fabrics, microbial or algal structures, and intercrystalline pore systems (Figures 5 and 6). These observations are consistent with the seismic and sedimentological interpretation that the platform margin provided a persistent high-energy depositional belt. Rather than considering the present reservoir porosity as entirely generated during late diagenesis, the preservation of an inherited sedimentary framework provides a more reasonable starting point for explaining the occurrence of effective reservoirs at extreme burial depth.

Vigorous hydrodynamic conditions promoted mud winnowing and the accumulation of relatively coarse carbonate grains, producing a grain-supported framework more resistant to compaction than micrite-rich deposits. Quantitative studies of carbonate compaction similarly show that porosity reduction varies with depositional texture and mud content [109]. The microbial and algal frameworks observed in the reservoir intervals may have further strengthened the original fabric [110,111]. Thus, the importance of the shoals lies not only in their initial pore space, but also in their capacity to preserve a pore-bearing framework during burial, consistent with the concentration of effective reservoirs documented by drilling and core observations.

Dolomitization represents the next important stage in this preservation history. Petrographic observations show widespread replacement by fine- to medium-crystalline dolomite and the occurrence of intercrystalline pores within the dolomitized framework (Figure 6). Early dolomitization could have contributed to the stabilization and preservation of the favorable depositional framework before extensive burial compaction and pressure solution. The recrystallization associated with dolomitization modified the original carbonate fabric and promoted the development of intercrystalline pore space, while the resulting dolomitized framework was more favorable for retaining reservoir space during subsequent burial [112–115]. The preservation of residual granular fabrics together

with intercrystalline pores in the Yudu dolomites is consistent with an early diagenetic stabilization process superimposed on a favorable depositional framework.

Dolomitization also contributed to the development and preservation of matrix-scale pore space [116–118]. Reorganization of carbonate minerals during dolomitization generated intercrystalline pores, which were widely observed in the thin sections. These pores should be considered as part of a coupled depositional–diagenetic evolution: the original shoal fabrics provided the initial pore framework, while dolomitization modified and locally stabilized this framework and generated additional intercrystalline pore space. Although individual pores are generally small, their cumulative distribution provides fluid-accessible space within the dolomitized framework and creates pathways that can later be enlarged by dissolution. The spatial variation in dolomitization further supports a relationship between depositional architecture and fluid circulation. Shoal complexes close to faults and the platform-margin slope break show stronger dolomitization than relatively low-energy intraplatform deposits, suggesting that the paleogeomorphic framework and fluid pathways were coupled during diagenesis. Faults associated with the Yudu rift trough may have facilitated the movement of Mg-bearing fluids and thereby promoted preferential dolomitization within structurally favorable shoal complexes [119,120]. This interpretation provides a link between the structural framework established during deposition and the subsequent diagenetic differentiation of the carbonate succession.

The importance of this coupling is also evident in the selective distribution of later dissolution. The original sedimentary fabrics and intercrystalline pore systems provided preferential pathways for subsequent fluids, and dissolution commonly affected algal grains, bioclasts, and oolitic particles rather than producing a completely fabric-independent pore system [121–123]. These relationships, documented in Figures 5 and 6, indicate that later modification inherited the architecture established during deposition and early diagenesis. The implication is significant for reservoir evolution: late fluids did not need to create an entirely new pore system in dense carbonate rock, but could instead enlarge and connect pore spaces that had survived earlier burial. This helps explain why reservoir-quality intervals are concentrated within particular shoal lithofacies rather than being distributed uniformly throughout the Cambrian carbonate succession.

The pore-evolution model summarizes this relationship. High-energy shoal deposition first established a favorable carbonate fabric and initial pore framework; early dolomitization subsequently modified and stabilized this framework while promoting the development of intercrystalline pore space; later fluids then enlarged and connected parts of the preserved pore system (Figure 9). This sequence explains why the present reservoir should not be regarded as either a purely primary-porosity reservoir or a reservoir created solely by late dissolution. The sedimentary fabric determined the initial distribution of pore space, whereas dolomitization influenced its preservation and subsequent accessibility to fluids. Later dissolution and fracturing acted on this inherited framework rather than replacing it completely.

Accordingly, the main significance of sedimentary–diagenetic coupling in the Yudu area is that it established a mechanism for preserving reservoir potential before the major phases of deep burial modification. High-energy shoals supplied a favorable primary depositional framework and initial pore system, while early dolomitization modified and stabilized this framework and promoted the development of intercrystalline pores. The preserved pore system subsequently provided pathways for later fluid–rock interaction, dissolution, and fracture-related modification. The most favorable reservoir prediction should therefore consider the coincidence of high-energy shoal facies and early dolomitization, particularly along fault-controlled platform-margin belts. This interpretation also places an important constraint on the role of later dissolution: dissolution was capable of

enhancing the reservoir only because a favorable and relatively stable pore framework had already survived the earlier stages of burial.

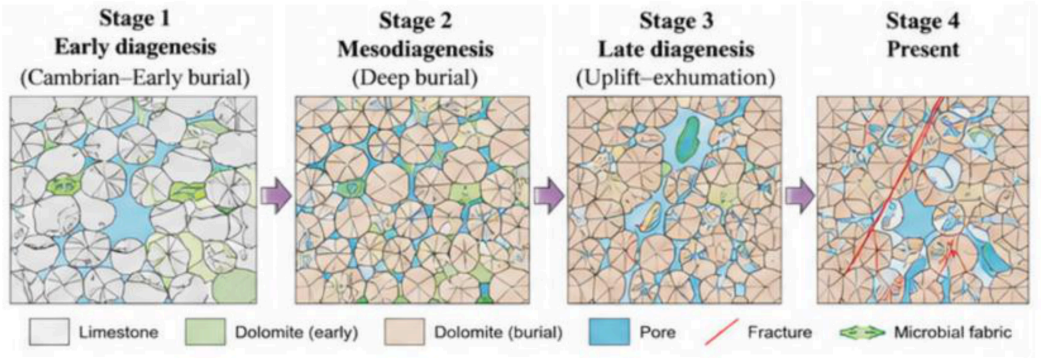


Figure 9. Schematic diagram of reservoir pore evolution in the Yudu area. High-energy platform-margin shoals developed along fault-controlled slope breaks and inherited paleogeomorphic highs, providing grain-supported and microbial carbonate frameworks with favorable primary pore space. Early dolomitization stabilized the carbonate framework and promoted the development and preservation of intercrystalline pores during burial. The inherited pore system subsequently provided preferential pathways for later dissolution and fluid–rock interaction, forming the initial reservoir framework for subsequent tectono-karstic modification.

6.3. Multi-Stage Tectono-Karstification and Reservoir Enhancement Mechanisms

The pore framework preserved through the combined effects of favorable depositional fabric and early diagenetic stabilization was subsequently modified by repeated dissolution and tectonic fracturing, producing the pore–fracture–vug systems characteristic of the Cambrian reservoirs in the Yudu area [124,125]. The observations show that dissolution pores, enlarged fractures, vugs, and fracture-associated cavities occur at both core and microscopic scales (Figures 4 and 7). These features are not evenly distributed through the carbonate succession. Instead, they are commonly associated with platform-margin shoals and structurally favorable intervals, indicating that the effectiveness of later reservoir modification depended strongly on the pre-existing sedimentary and structural framework. The present reservoir architecture therefore reflects successive modification of an inherited pore system rather than the product of a single episode of karstification.

Early dissolution probably began before deep burial during episodes of exposure and relative sea-level fall. In shallow platform-margin settings, meteoric fluids could penetrate exposed carbonate surfaces and preferentially dissolve unstable grains and microbial or algal components [126,127]. The fabric-selective dissolution features observed in thin sections, including the dissolution of algal grains, bioclasts, and oolitic particles, are consistent with this process. These early dissolution events may not have generated the largest proportion of the present reservoir volume, but they were important because they introduced secondary pore space and increased the accessibility of the carbonate framework to later fluids. In this respect, early dissolution acted mainly as a preparatory stage for subsequent reservoir enhancement.

Unconformity-related karstification represents a later and potentially more extensive stage of meteoric modification. Core observations include irregular dissolution cavities, collapse-related textures, red-stained alteration, and fracture-associated vugs near relevant stratigraphic boundaries (Figure 4). These features provide direct evidence that exposure-related fluids modified the Cambrian carbonates beyond the scale of individual grains. The distribution of these features also suggests a structural control: elevated platform-margin shoals were more readily exposed, while faults could have provided pathways for downward fluid penetration. Consequently, karstification was favored where paleogeomorphic relief,

reservoir-prone facies, and structural conduits coincided. This relationship is important because it links the observed dissolution features to the fault-controlled paleogeomorphology.

With progressive burial, basinal and organic acid-bearing fluids could further modify the inherited pore system [127–132]. Crosscutting dissolution pores and fracture-associated cavities observed in the thin sections and cores (Figure 7) indicate that burial dissolution mainly enlarged and connected pre-existing pores rather than generating an entirely new pore system. Repeated reactivation of rift-related faults further enhanced this process by providing preferential pathways for fluid migration [128–130]. Fracture enlargement by dissolution produced vugs and fracture–cavity systems (Figures 4 and 7), making fracture–pore connectivity more important to reservoir effectiveness than the abundance of any single pore type [131–133].

The spatial association between major faults and dissolution-enhanced reservoirs further supports this interpretation. Intervals close to major structural zones commonly display stronger fracture development and more complex pore–fracture–vug assemblages than structurally distal carbonate rocks [134–136]. Long-lived fault activity could have repeatedly reopened fluid pathways during different stages of burial and tectonic reactivation. However, the relationship should not be interpreted as a simple increase in reservoir quality with proximity to every fault. Intense dissolution and fracturing can also generate localized cavities, collapse breccias, or strongly heterogeneous pore systems. Thus, faults are best regarded as fluid and deformation conduits whose reservoir effect depends on the underlying carbonate facies and diagenetic history.

The superposition of these processes is summarized in Figure 10. The model begins with high-energy shoal deposition and early preservation of pore space, followed by dissolution, karstification, fracture development, and fracture-assisted dissolution. The important feature of this model is the sequential relationship among the processes. Early pore systems provided the substrate for later dissolution; exposure and unconformity processes enlarged that pore system; burial fluids modified previously developed pores; and tectonic fractures connected otherwise isolated pore domains. The final pore–fracture–vug network consequently represents the cumulative product of several geological stages rather than a single late-stage event.

The resulting reservoir heterogeneity reflects the uneven superposition of favorable shoal facies, preserved intercrystalline pores, paleogeomorphic relief, and fault-related fluid pathways. Reservoir prediction should therefore evaluate these factors together rather than using fault proximity or karst intensity as independent criteria. In the Yudu area, tectono-karstification was most effective where structurally focused fluid flow acted on a pre-existing pore-bearing shoal framework.

Taken together, the evidence supports a model in which reservoir enhancement proceeded through repeated modification of pre-existing pore systems. Early dissolution and unconformity karstification introduced secondary pore space, burial fluids enlarged selected pores, and tectonic fractures provided the principal conduits for fluid migration and pore connection. The resulting reservoir is therefore best described as a tectono-karstic pore–fracture–vug system developed on a sedimentary–diagenetic framework, rather than as either a purely karst-controlled or purely fracture-controlled reservoir. This distinction is important for predicting effective ultra-deep Cambrian reservoirs because the most favorable intervals therefore require a favorable primary depositional framework that has been sufficiently preserved or modified during early diagenesis, together with a subsequent history of focused tectono-fluid modification.

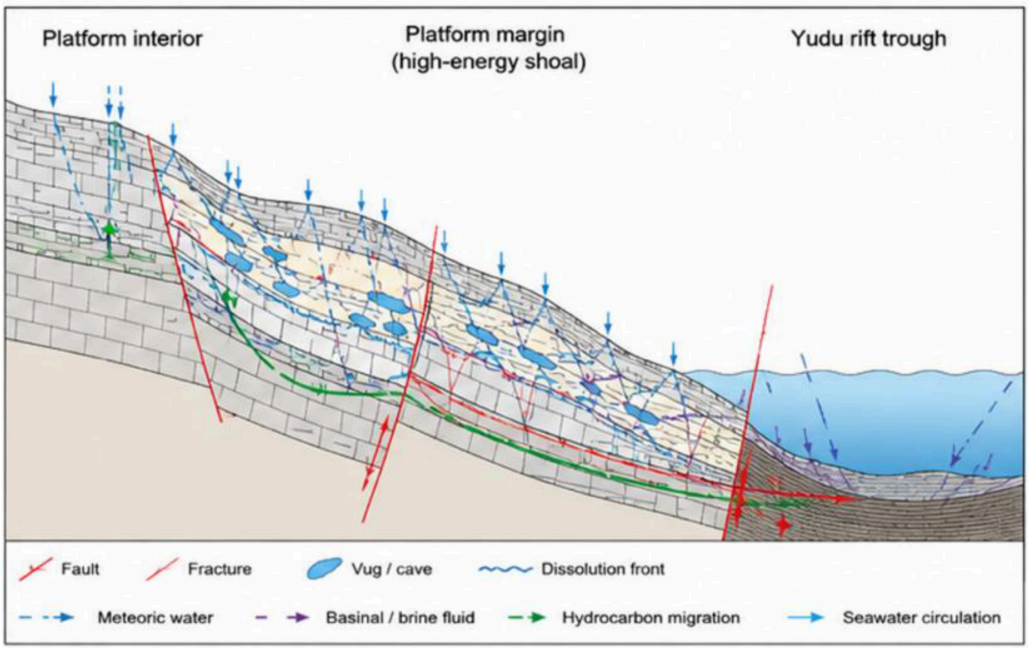


Figure 10. Schematic diagram of reservoir formation mechanism in the Yudu area. The preserved pore framework was progressively modified by early dissolution, unconformity-related karstification, burial-stage fluid–rock interaction, and tectonic fracturing. Faults acted as preferential conduits for fluid migration, while fracture-associated dissolution enlarged and interconnected pre-existing pores. The superposition of dissolution, fractures, and vugs ultimately produced an interconnected pore–fracture–vug reservoir system, particularly within platform-margin shoal facies adjacent to long-lived fault zones.

The reservoir-forming model proposed for the Yudu area is broadly consistent with recent studies of deep carbonate systems in the Tarim Basin, while also highlighting the importance of the inherited depositional framework [137–139]. Wang et al. [140] demonstrated that the distribution of deep carbonate reservoirs in the southern Tahe Oilfield was controlled by the coupling between multistage fault activity and diagenetic fluids, with faults providing preferential pathways for dissolution and hydrothermal fluid migration. This observation provides a useful regional comparison for the Yudu area, where the close association between faults, dissolution features, and fracture–vug systems likewise indicates that structural reactivation played an important role in reservoir modification. However, the Yudu case differs in that the later tectono-fluid processes appear to have acted preferentially on platform-margin shoal facies that had already been stabilized by early dolomitization. This interpretation is also compatible with the quantitative compaction study of carbonate successions from offshore Western Australia, which demonstrated that porosity reduction is strongly influenced by depositional texture, mud content, and mineralogy, with grain-supported fabrics and dolomitization producing deviations from simple depth-dependent compaction trends [141–144]. Thus, the preservation of reservoir space in Yudu cannot be attributed to faulting or dissolution alone; it reflects the interaction between an initially favorable shoal framework, early diagenetic stabilization, and later structural-fluid modification. More broadly, recent geochemical work on Lower Cambrian organic-rich strata in the Tarim Basin emphasized strong spatial and stratigraphic heterogeneity in depositional conditions and source-rock development, controlled by paleogeography, redox conditions, hydrothermal input, and terrigenous supply [55,109,145]. Although that study focused on source-rock evolution rather than carbonate reservoir architecture, its recognition of strong basin-scale heterogeneity reinforces the need to evaluate reservoir and source conditions within their specific paleogeographic framework rather than assuming uniformity across

the Tarim Basin. Taken together, these comparisons support a process-based model in which paleogeography establishes the depositional template, early diagenesis determines the preservation potential of the pore framework, and later fault-controlled fluid circulation governs reservoir enhancement and connectivity.

6.4. Coupling Between Rift-Related Hydrocarbon Kitchens and Platform-Margin Reservoirs

The spatial association between the hydrocarbon kitchens interpreted within the Yudu rift trough and the adjacent platform-margin shoal reservoirs provides an important basis for interpreting the hydrocarbon accumulation pattern in the study area. In contrast to conventional carbonate systems involving long-distance migration, the Cambrian system in the Yudu area may have favored a near-source accumulation pattern, based on the close spatial relationship between the rift trough, reservoir-prone shoals, fault systems, and observed hydrocarbon occurrences [48,146,147]. This interpretation is based primarily on the observed structural and spatial relationships; direct geochemical evidence linking the source rocks to the reservoir hydrocarbons and direct constraints on the timing of hydrocarbon charging are not currently available. Therefore, the near-source model should be regarded as a geological interpretation rather than a fully demonstrated source–reservoir correlation (Figure 11).

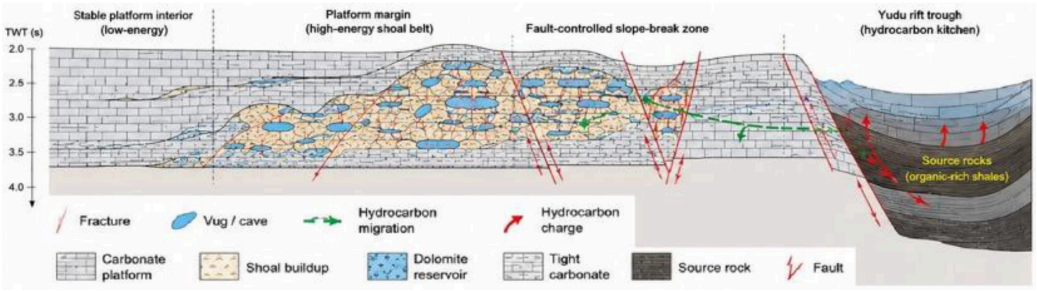


Figure 11. Schematic diagram of hydrocarbon accumulation regularity in the Yudu area. Cambrian source rocks developed within the Yudu rift trough provided hydrocarbons to adjacent platform-margin reservoirs. Fault systems acted as long-lived conduits connecting the source kitchen with structurally favorable shoal reservoirs and also controlled the development and enhancement of fracture–vug networks. Hydrocarbons migrated from the rift-related source kitchen into adjacent dolomitized platform-margin shoals and accumulated preferentially where favorable reservoir facies, enhanced pore–fracture–vug connectivity, and effective structural migration pathways overlapped. The model highlights the coupled control of source distribution, platform-margin reservoir development, fault-controlled migration, and structural preservation on Cambrian hydrocarbon accumulation.

The Cambrian intracratonic extensional framework established the Yudu rift trough as a site favorable for organic-rich sedimentation and the adjacent platform margin as a setting for high-energy carbonate accumulation [148,149]. This paleogeographic configuration placed potential source-rock intervals and reservoir-prone shoals in close spatial proximity and therefore provides a geological basis for considering relatively short migration pathways. Faults and associated fractures may have provided potential vertical and lateral pathways between the rift trough and adjacent shoal reservoirs during later burial evolution [146,150,151]. However, the extent to which these structures directly connected specific source intervals with individual reservoirs cannot be resolved from the present dataset.

Drilling data indicate widespread hydrocarbon shows, overflow phenomena, abnormal pressure coefficients, and considerable gas-column heights within Cambrian platform-margin reservoirs. These observations demonstrate the occurrence of hydrocarbon accumulations within the study area and are spatially consistent with the proximity of the reservoirs to the Yudu rift trough. However, the present dataset does not directly quantify hydrocarbon charging intensity, identify the specific source intervals responsible for the

accumulated hydrocarbons, or constrain whether hydrocarbon supply was sustained over particular geological time intervals. Similarly, the observed abnormal pressure coefficients cannot, on their own, establish a direct relationship between overpressure development and hydrocarbon generation or charging.

Under ultra-deep burial conditions, abnormal fluid pressure may influence effective stress, and in some geological settings, affect porosity evolution and the fracture behavior [152–154]. In the Yudu area, abnormal pressure coefficients occur in association with some hydrocarbon-bearing and fracture–vuggy reservoir intervals. This spatial association may be relevant to the evolution of the reservoir–fluid system; however, the present data do not allow for the specific origin, timing, or reservoir-preservation effect of overpressure to be determined. Accordingly, a direct causal relationship between overpressure, hydrocarbon charging, and long-term preservation of reservoir space is not inferred here.

Fault systems associated with the Yudu rift trough provide another important structural element in the proposed accumulation model. These faults influenced platform-margin sedimentation and subsequently generated fracture systems that may have affected fluid circulation during burial evolution. Their spatial association with hydrocarbon-bearing reservoirs suggests that faults and related fractures could have served as potential migration pathways. However, the present dataset does not directly establish the direction, volume, timing, or efficiency of hydrocarbon migration along individual fault systems.

Fault reactivation during multiple tectonic stages may have repeatedly modified fracture networks and influenced fluid circulation. Bitumen-bearing fractures and mineral-filled or dissolution-enlarged fractures observed in the cores and thin sections indicate a complex history of fluid movement and fracture evolution. Although these features are compatible with multiple episodes of fluid activity, they do not independently constrain the number, timing, or source of hydrocarbon charging events.

Tectonic activity and burial fluid circulation may also have contributed to dissolution within the platform-margin reservoirs. Organic acid-bearing fluids generated during source-rock maturation can promote carbonate dissolution in deep petroleum systems [155–157], and such processes represent one possible mechanism for burial-stage pore enlargement in the Yudu area. However, the composition and origin of the fluids responsible for the observed dissolution were directly constrained in the present study. The contribution of hydrocarbon-related acidic fluids to reservoir enhancement should therefore be regarded as a possible diagenetic mechanism rather than a demonstrated process.

Another feature of the Yudu area is the spatial association between hydrocarbon-bearing reservoirs and the platform-margin shoal belt adjacent to the rift trough. Exploration results indicate that productive reservoirs are mainly concentrated along this belt rather than in more distal intraplatform settings. This distribution is consistent with the proposed near-source accumulation model, but reservoir occurrence may also reflect differences in depositional facies, diagenetic modification, structural connectivity, and trap preservation. Therefore, the present data do not allow the relative contribution of proximity to potential source rocks to be separated from these other geological controls, nor can reduced hydrocarbon charging in more distal areas be directly demonstrated.

The source–reservoir coupling model recognized in the Yudu area differs somewhat from traditional long-distance migration models commonly proposed for cratonic carbonate basins. In many classical petroleum systems, hydrocarbons generated in deep basinal depressions migrate over long distances into structurally elevated traps. In contrast, the Yudu system can be interpreted as a more spatially integrated tectono-sedimentary framework in which potential source intervals, reservoir-prone facies, fault systems, and structural traps occur within the same rift-controlled platform-margin setting. This configuration provides a geological basis for considering relatively short migration pathways,

although the efficiency and timing of hydrocarbon transfer cannot be quantified from the present dataset.

The coupling between hydrocarbon kitchens and platform-margin reservoirs also has important implications for reservoir heterogeneity and hydrocarbon distribution. Areas characterized by stronger fault development and structural connectivity may have experienced more extensive fluid circulation and tectono-diagenetic modification. These areas commonly display better-developed dissolution features, bitumen occurrence, and complex fracture–vug networks. Although such spatial relationships are compatible with the proposed accumulation model, they do not by themselves demonstrate stronger hydrocarbon charging or direct connectivity to specific source intervals. Conversely, structurally isolated shoal bodies may preserve poorer reservoir connectivity and weaker hydrocarbon saturation despite possessing similar depositional facies characteristics.

From a broader basin evolution perspective, the Yudu petroleum system demonstrates how intracratonic rifting can simultaneously control source rock development, platform-margin sedimentation, reservoir enhancement, and hydrocarbon accumulation within deep carbonate systems. The Yudu rift trough not only created favorable conditions for organic matter enrichment during the Cambrian, but also established the tectono-paleogeomorphic framework necessary for subsequent reservoir development and hydrocarbon migration. Thus, the entire petroleum system evolution can be regarded as a long-term product of intracratonic extensional tectonism.

This understanding has significant exploration implications for the Cambrian carbonate system throughout the Tarim Basin. It suggests that future exploration should prioritize fault-controlled platform-margin shoal belts located adjacent to major Cambrian hydrocarbon kitchens. Such areas combine several geological factors that are favorable for hydrocarbon accumulation including: (1) high-energy shoal facies with greater reservoir potential; (2) favorable conditions for dolomitization and dissolution; (3) well-developed tectonic fractures and structural connectivity; and (4) close spatial association with potential Cambrian source-rock intervals. These factors provide useful criteria for identifying prospective exploration targets, although the effectiveness and timing of hydrocarbon migration require further geochemical and chronological constraints. The superposition of these factors greatly increases the probability of preserving large-scale effective ultra-deep reservoirs and commercial hydrocarbon accumulations.

Overall, the Cambrian petroleum system in the Yudu area can be interpreted as a rift-controlled, near-source accumulation system, in which the spatial association of the rift trough, platform-margin reservoirs, and fault networks provides a coherent geological framework for hydrocarbon migration and accumulation. Although the present dataset does not directly establish source–reservoir geochemical correlation or the precise timing of hydrocarbon charging, the spatial coincidence of favorable reservoir facies, major faults, and hydrocarbon occurrences supports this interpretation. This model provides a useful framework for evaluating similar fault-controlled platform-margin carbonate systems in the Tarim Basin, while future geochemical correlation and fluid-inclusion or geochronological studies are required to further test the proposed migration and charging history.

6.5. Genetic Model and Exploration Implications

The Yudu-Gucheng area hosts ultra-deep Cambrian dolomite reservoirs buried to 8.3–8.7 km, representing a typical example of fault-controlled platform-margin shoal reservoirs within intracratonic rift-trough settings of the Tarim Basin [158]. Our integrated analysis indicates that reservoir development and preservation resulted from the successive and superimposed effects of synsedimentary fault-controlled paleogeomorphology, high-energy shoal deposition, early diagenetic modification and dolomitization, and multistage

tectono-karstic alteration. In this framework, the structural framework first controlled the location and development of platform-margin shoals, whereas the resulting depositional fabrics provided favorable initial pore space. Early diagenetic processes, particularly dolomitization, subsequently modified and stabilized parts of the carbonate framework and promoted the development and preservation of intercrystalline pore space. During later burial and tectonic evolution, dissolution and fault-related fluid flow further enlarged and interconnected the preserved pore system, ultimately producing the present pore–fracture–vug reservoir architecture.

Globally, many Cambrian–Ordovician deep carbonate reservoirs are conventionally interpreted to have been strongly influenced by eustatic sea-level fluctuations and regional epeirogenic movements [22]. In the Yudu area, however, the structural framework exerted an important control on the spatial distribution of platform-margin shoals. Synsedimentary inherited faults generated persistent slope-break zones that focused carbonate accumulation and localized the development and stacking of high-energy shoal complexes, even under changing relative sea-level conditions [8]. The resulting shoal deposits provided favorable depositional fabrics and initial pore frameworks for subsequent reservoir development. Their preservation during burial was not controlled by depositional texture alone. Rather, early diagenetic modification, particularly dolomitization, played an important role in stabilizing the carbonate framework and reorganizing the pore system before subsequent burial, dissolution, and tectonic modification. This interpretation is consistent with observations from the Tahe Oilfield, where fault-related fluid flow and diagenetic processes substantially modified pre-existing carbonate reservoirs [66]. The Yudu example therefore suggests that later tectono-karstic processes preferentially modified carbonate intervals in which favorable depositional fabrics and early diagenetic stabilization had already provided a suitable framework for reservoir preservation, rather than generating effective reservoir space independently within the entire carbonate succession.

For regional exploration perspective, fault-related slope-break zones adjacent to intracratonic rift troughs should therefore receive particular attention in the search for ultra-deep carbonate reservoirs in the Tarim Basin. However, the presence of a slope-break belt alone does not necessarily indicate the development of a high-quality reservoir. Favorable targets require the superposition of several geological conditions, including well-developed platform-margin high-energy shoal deposits, preservation or modification of favorable depositional fabrics through early diagenesis and dolomitization, and subsequent fault-related fluid activity capable of enhancing the pore system through dissolution and fracture development [17,68]. This sequence emphasizes that exploration should not simply target structural highs or fault zones, but should identify areas where depositional facies, early diagenetic evolution, and later tectono-fluid activity are spatially superimposed.

Limitations of the present study should also be noted. The current seismic resolution limits quantitative assessment of the relative contributions of tectonic paleogeomorphology and eustatic sea-level change to shoal migration and stacking. In addition, the available dataset does not allow for the relative importance and precise timing of individual diagenetic and tectono-fluid events to be quantitatively constrained. Further work combining high-resolution sequence stratigraphy, numerical subsidence modeling, detailed petrographic and geochemical characterization, and more tightly constrained diagenetic and fluid-evolution datasets would help resolve these issues. Nevertheless, the genetic model proposed here provides a geological framework for understanding how depositional architecture, early diagenetic stabilization, and subsequent tectono-karstic modification interact to produce and preserve effective ultra-deep dolomite reservoirs. It also provides a basis for identifying analogous reservoir systems developed along structurally controlled platform

margins in other intracratonic rift settings of the Tarim Basin and comparable ancient cratonic basins.

7. Conclusions

1. Cambrian platform-margin high-energy shoals in the Yudu area developed preferentially along fault-controlled slope breaks and inherited paleogeomorphic highs associated with the Yudu rift trough. Progradational seismic architectures and superposed shoal complexes indicate that synsedimentary tectonism exerted a persistent control on the location and development of the platform-margin depositional system.
2. High-energy shoal deposits provided the primary framework for effective Cambrian dolomite reservoirs. Grain-supported and microbial carbonate fabrics, together with early dolomitization, favored preservation of the inherited pore framework during burial and generated intercrystalline pore systems. Reservoir-prone intervals are concentrated mainly within platform-margin shoal belts adjacent to the rift trough.
3. Reservoir quality was subsequently enhanced by multistage dissolution and tectonic fracturing. Early and unconformity-related dissolution, burial-stage fluid–rock interaction, and fault-related fracture development progressively modified the preserved pore system, producing interconnected pore–fracture–vug networks. The most favorable reservoirs occur where high-energy shoal facies, preserved pore space, and long-lived fault-controlled fluid pathways overlap.
4. The Yudu Cambrian carbonate system represents a fault-controlled tectono-sedimentary–diagenetic petroleum system in which synsedimentary tectonism established the depositional framework, early diagenesis preserved reservoir potential, and later tectono-fluid activity enhanced reservoir connectivity and hydrocarbon migration. The spatial association of rift-related source kitchens, platform-margin shoal reservoirs, and long-lived faults provides a favorable configuration for near-source hydrocarbon accumulation and identifies fault-controlled platform-margin belts as important targets for the further exploration of ultra-deep Cambrian carbonates in the Tarim Basin.

This study establishes a tectono-sedimentary-diagenetic genetic model for Cambrian platform-margin dolomite reservoirs and provides important insights into the prediction of favorable exploration targets in deep and ultra-deep carbonate systems of similar basins, such as the Sichuan Basin and Ordos Basin.

Author Contributions: Writing—original draft preparation, Y.L., J.L., B.Y., R.D., Y.Z. (Yong Zhong); writing—review and editing, R.X., Y.Z. (Yuangao Zhang), X.W., Y.C. and S.Z.; Conceptualization, Y.L. and J.L.; methodology, R.X.; software, B.Y.; validation, R.D., Y.Z. (Yuangao Zhang) and X.W.; investigation, Y.Z. (Yong Zhong), Y.C. and S.Z. All authors have read and agreed to the published version of the manuscript.

Funding: The research and the APC were funded by the National Oil and Gas Special Project: Study on Marine Hydrocarbon Enrichment Regularity and Large-Scale Reserve Increase in Platform-Basin Area (No. 2025ZD1400506) and the China Petroleum Science and Technology Project: Integrated Research and Strategic Prospect Selection of the Tarim Basin (No. 2025YQXN20202).

Data Availability Statement: The data presented in this study are available in the article.

Conflicts of Interest: Authors Yang Liu, Bo Yan, Rui Deng, Xiandong Wang, Yong Zhong, Shan Zhao were employed by the company Exploration and Development Research Institute, PetroChina Daqing Oilfield Company Limited, which had no input in the research processes or results presented. The remaining authors declare that the research was conducted in the absence of any commercial or financial relationships that could be construed as a potential conflict of interest.

References

1. Ma, Y.; Cai, X.; Yun, L.; Li, Z.; Li, H.; Deng, S.; Zhao, P. Practice and theoretical and technical progress in exploration and development of Shunbei ultra-deep carbonate oil and gas field, Tarim Basin, NW China. *Pet. Explor. Dev.* **2022**, *49*, 1–20. [CrossRef]
2. Yang, H.; Wang, C.; Yang, X.; Zhang, Z.; Guo, X.; Sun, C.; Lyu, X.; Liu, J. Technological progress and scientific significance of the drilling of the ten-thousand-meter ultra-deep well TK1, Tarim Basin, NW China. *Pet. Explor. Dev.* **2025**, *52*, 1329–1339. [CrossRef]
3. Chen, L.; Jiang, Z.; Sun, C.; Ma, B.; Su, Z.; Wan, X.; Han, J.; Wu, G. An overview of the differential carbonate reservoir characteristic and exploitation challenge in the Tarim Basin (NW China). *Energies* **2023**, *16*, 5586. [CrossRef]
4. Du, J.; Pan, W. Accumulation conditions and play targets of oil and gas in the Cambrian subsalt dolomite, Tarim Basin, NW China. *Pet. Explor. Dev.* **2016**, *43*, 360–374. [CrossRef]
5. Wei, G.; Zhu, Y.; Zheng, J.; Yu, G.; Ni, X.; Yan, L.; Tian, L.; Huang, L. Tectonic-lithofacies paleogeography, large-scale source-reservoir distribution and exploration zones of Cambrian subsalt formation, Tarim Basin, NW China. *Pet. Explor. Dev.* **2021**, *48*, 1289–1303. [CrossRef]
6. Guan, S.; Zhang, C.; Ren, R.; Zhang, S.; Wu, L.; Wang, L.; Ma, P.; Han, C. Early Cambrian syndepositional structure of the northern Tarim Basin and a discussion of Cambrian subsalt and deep exploration. *Pet. Explor. Dev.* **2019**, *46*, 1141–1152. [CrossRef]
7. Hu, Z.; Feng, F.; Fang, C.; Cao, Z.; Wang, T.; Guo, K.; Li, Y.; Wang, S. Segmented evolution and exploration targets of the Cambrian platform margin in the Manxi area, Tarim Basin. *Energy Geosci.* **2025**, *6*, 100367. [CrossRef]
8. Zhang, K.; You, X.; Wu, Y.; Zhao, Y.; Wang, J. The main controlling factors on the evolution of the Cambrian carbonate platform in the Tarim Basin and its implications for the distribution of ultra-deep dolomite reservoirs. *Minerals* **2023**, *13*, 245. [CrossRef]
9. Li, S.; Li, Y.; Peng, S.; Hao, Y.; Zhang, J.; Wang, J.; Xu, X. Tectonic–Sedimentary Differentiation of Cratonic Basins in China and Its Controlling Effects on the Development of Large-Scale Carbonate Reservoirs. In *Petroleum Geology and Exploration of Deep Marine Strata in China*; Springer: Berlin/Heidelberg, Germany, 2026; pp. 57–87.
10. Xu, X.; Chen, Q.; Chu, C.; Li, G.; Liu, C.; Shi, Z.J. Tectonic evolution and paleokarstification of carbonate rocks in the Paleozoic Tarim Basin. *Carbonates Evaporites* **2017**, *32*, 487–496. [CrossRef] [PubMed]
11. Ingersoll, R.V. Tectonics of sedimentary basins, with revised nomenclature. In *Tectonics of Sedimentary Basins: Recent Advances*; Wiley: Hoboken, NJ, USA, 2011; pp. 1–43.
12. Yin, H. A Comparative Study of Silicified Rock Reservoir in Shunnan 4 well of Tarim Basin with Hydrothermal Chert Reservoir of Parkland Gas Field in Western Canada Sedimentary Basin. Master's Thesis, University of Regina, Regina, SK, Canada, 2018.
13. Busby, C.; Pérez, A.A. *Tectonics of Sedimentary Basins: Recent Advances*; Wiley: Hoboken, NJ, USA, 2011.
14. Zhang, J.; Hu, M.; Feng, Z.; Li, Q.; He, X.; Zhang, B.; Yan, B.; Wei, G.; Zhu, G.; Zhang, Y. Types of the Cambrian platform margin mound-shoal complexes and their relationship with paleogeomorphology in Gucheng area, Tarim Basin, NW China. *Pet. Explor. Dev.* **2021**, *48*, 110–122. [CrossRef]
15. Dong, C.; Hu, C.; Quaye, J.A.; Wang, X.; He, G. Marine carbonate shoal reservoirs: Review and perspectives. *Int. Geol. Rev.* **2026**, *68*, 1001–1026. [CrossRef]
16. Liu, Y.; Hu, M.; Zhang, S. Types, structural evolution difference and petroleum geological significance of Cambrian–Ordovician carbonate platforms in Gucheng–Xiaotang area, Tarim Basin, NW China. *Pet. Explor. Dev.* **2022**, *49*, 1019–1032. [CrossRef]
17. Lambiase, J.J.; Morley, C.K. Hydrocarbons in rift basins: The role of stratigraphy. *Philos. Trans. R. Soc. A Math. Phys. Eng. Sci.* **1999**, *357*, 877–900. [CrossRef]
18. Zhang, S.; Su, J.; Wang, X.; Ma, S. Sedimentary Environments of Cambrian–Ordovician Source Rocks and Ultra-deep Petroleum Accumulation in the Tarim Basin. *Acta Geol. Sin.* **2022**, *96*, 1259–1276. [CrossRef]
19. Wu, L.; Guan, S.; Ren, R.; Wang, X.; Yang, H.; Jin, J.; Zhu, G. The characteristics of Precambrian sedimentary basin and the distribution of deep source rock: A case study of Tarim Basin in Neoproterozoic and source rocks in Early Cambrian, Western China. *Pet. Explor. Dev.* **2016**, *43*, 988–999. [CrossRef]
20. Zeng, Q.; He, T.; Zhao, Y.; Zhang, K.; Wen, Z.; Xu, Y.; He, J.; Tian, W.; Lu, S.; Cheng, W. Geochemical characteristic of different-lithofacies source rocks and its implications for ultradeep hydrocarbon exploration in the lower cambrian Yuertus formation, Tarim basin. *Sci. Rep.* **2025**, *15*, 24071. [CrossRef] [PubMed]
21. Zhu, Y.; Zheng, J.; Cao, P.; Qiao, Z.; Yu, G.; Liu, L.; Huang, L. Tectonic-Lithofacies paleogeography and sizeable reservoir potential in the Early Cambrian postrift depressed carbonate ramp, Tarim Basin, NW China. *Lithosphere* **2021**, *2021*, 8804537. [CrossRef]
22. Zhang, K.; You, X.; Ma, T.; Wang, J.; Wu, Y.; Lu, Y.; Zhang, S. The Main Controlling Factors of the Cambrian Ultra-Deep Dolomite Reservoir in the Tarim Basin. *Minerals* **2024**, *14*, 775. [CrossRef]
23. Wei, G.; Zhu, Q.; Yang, W.; Zhang, C.; Mo, W. Cambrian faults and their control on the sedimentation and reservoirs in the Ordos Basin, NW China. *Pet. Explor. Dev.* **2019**, *46*, 883–895. [CrossRef]
24. Yuan, H.; Chen, S.; Dai, K.; Guo, X.; Kong, L.; Feng, N.; Zhao, H.; Yang, W.J. Distribution of Cambrian Source Rock controlled by the inherited paleotopography on the precambrian basement in the Tarim Basin, NW China. *Front. Earth Sci.* **2022**, *10*, 864082. [CrossRef]

25. Shen, L.; Liao, Q.; Chen, Y.; Han, Y.; Zhu, Z.; Shi, J.; Wu, Q. Restoration of Cambrian Paleogeomorphology and Its Geological Significance in the Tabei Area, Tarim Basin. *ACS Omega* **2025**, *10*, 59629–59641. [CrossRef] [PubMed]
26. James, N.P.; Mountjoy, E.W. Shelf-slope break in fossil carbonate platforms: An overview. In *The Shelfbreak: Critical Interface on Continental Margins*; SEPM, Society for Sedimentary Geology: Tulsa, OK, USA, 1983.
27. Wei, W.; Liu, H.; Wang, D.; Hu, X.; Tan, L.; Liu, B.; Yin, C.; Yang, W.-J. Sedimentary characteristics and evolutionary processes of platform margin shoals of the Permian Maokou Formation in the Jiange-Yuanba area, Sichuan Basin, SW China. *Facies* **2026**, *72*, 15. [CrossRef]
28. Tan, X.; Liu, H.; Li, L.; Luo, B.; Liu, X.; Mou, X.; Nie, Y.; Xi, W. Primary intergranular pores in oolitic shoal reservoir of lower triassic feixianguan formation, Sichuan Basin, Southwest China: Fundamental for reservoir formation and retention diagenesis. *J. Earth Sci.* **2011**, *22*, 101–114. [CrossRef]
29. Jiang, L.; Cai, C.; Worden, R.H.; Crowley, S.F.; Jia, L.; Zhang, K.; Duncan, I.J.J. Multiphase dolomitization of deeply buried Cambrian petroleum reservoirs, Tarim Basin, north-west China. *Sedimentology* **2016**, *63*, 2130–2157. [CrossRef]
30. Wu, J.-p.; Cheng, X.-d.; Fan, L.-y.; Hab, G.-q.; Tai, U.-m.; Li, Y. Comprehensive Prediction of Carboniferous KT-II Shoal Thin Reservoirs in the Eastern Margin of the Pre-Caspian Basin. In *Proceedings of International Field Exploration and Development Conference 2022*; Springer: Singapore, 2022; pp. 495–510.
31. Wu, Y.; Li, Y.; Zhang, Z.; Sun, L. Effect of water pressure and expulsion on hydrocarbon generation of kerogen under semi-closed conditions. *Arab. J. Geosci.* **2021**, *14*, 1333. [CrossRef]
32. Liu, H.; Jiang, Y. Hydrocarbon Accumulation and the Formation of Hydrocarbon Reservoirs. In *Petroleum Geology*; Springer: Berlin/Heidelberg, Germany, 2025; pp. 305–388.
33. Zhu, G.; Cao, Y.; Yan, L.; Yang, H.; Sun, C.; Zhang, Z.; Li, T.; Chen, Y. Potential and favorable areas of petroleum exploration of ultra-deep marine strata more than 8000 m deep in the Tarim Basin, Northwest China. *J. Nat. Gas. Geosci.* **2018**, *3*, 321–337. [CrossRef]
34. Xia, J.; Zhong, Z.; Huang, S.; Luo, C.; Lou, H.; Chang, H.; Li, X.; Wei, L.J. The proto-type basin and tectono-paleogeographic evolution of the Tarim basin in the Late Paleozoic. *Front. Earth Sci.* **2023**, *11*, 1097101. [CrossRef]
35. Yang, H.; Zhou, J.; Ma, J.; Cui, X. Aromatic carotenoids and their aryl isoprenoid derivatives in the early Paleozoic rocks and crude oils of the Tarim Basin, China. *Org. Geochem.* **2025**, *202*, 104950. [CrossRef]
36. Zhang, C.-L.; Zou, H.-B.; Ye, X.-T.; Chen, X.-Y. Tectonic evolution of the West Kunlun Orogenic Belt along the northern margin of the Tibetan Plateau: Implications for the assembly of the Tarim terrane to Gondwana. *Geosci. Front.* **2019**, *10*, 973–988. [CrossRef]
37. Xiao, X.; Liu, X.; Gao, R.; Kao, H.; Luo, Z. Collision tectonics between the Tarim Block (Basin) and the northwestern Tibet Plateau: New observations from a multidisciplinary geoscientific investigation in the western Kunlun Mountains. *Acta Geol. Sin.* **2001**, *75*, 126–132. [CrossRef]
38. Zhang, C.-L.; Zou, H.-B.; Li, H.-K.; Wang, H.-Y. Tectonic framework and evolution of the Tarim Block in NW China. *Gondwana Res.* **2013**, *23*, 1306–1315. [CrossRef]
39. Ren, R.; Guan, S.; Wu, L.; Zhu, G. Evolution of the Neoproterozoic rift basins and its implication for oil and gas exploration in the Tarim Basin. *Pet. Res.* **2018**, *3*, 66–76. [CrossRef]
40. Liu, W.; Zou, Y.; Tian, W.; Jiang, T.; Yan, W.; Nance, R.D.; Zhou, X. The origin and tectonic evolution of the late Neoproterozoic rift basin in the Tarim Craton, NW China. *J. Asian Earth Sci.* **2024**, *262*, 106011. [CrossRef]
41. Liu, J.; Wu, G.; Tang, Q.; Wu, Y.; Zhang, W.; Zhao, Z. Effects of Intracratonic Strike-slip Fault on the Differentiation of Carbonate Microfacies: A Case Study of a Permian Platform Margin in the Sichuan Basin (SW China). *Acta Geol. Sin.* **2024**, *98*, 936–954. [CrossRef]
42. Xu, Q.; Yang, W.; Wen, L.; Li, S.; Luo, B.; Xiao, D.; Qiao, Z.; Liu, S.; Li, M.; Guo, J.; et al. Controlling effects of the Mid-Permian multistage slope-break zones on paleogeomorphology and large-scale shoals in the Sichuan Basin, SW China. *Pet. Explor. Dev.* **2025**, *52*, 952–967. [CrossRef]
43. Liu, H.; Lin, C.-S.; Guo, R.-B.; Zhu, M.; Cui, Y.-Q. Characteristics of the Paleozoic slope break system and its control on stratigraphic-lithologic traps: An example from the Tarim Basin, western China. *J. Palaeogeogr.* **2015**, *4*, 284–304. [CrossRef]
44. Zhang, M.; Lin, C. Syndepositional structures and structural slope-break zones. In *Seismic Geology and Basin Analysis*; Elsevier: Amsterdam, The Netherlands, 2024; pp. 95–107.
45. Feng, Y.; Jiang, S.; Hu, S.; Li, S.; Lin, C.; Xie, X. Sequence stratigraphy and importance of syndepositional structural slope-break for architecture of Paleogene syn-rift lacustrine strata, Bohai Bay Basin, E. China. *Mar. Pet. Geol.* **2016**, *69*, 183–204. [CrossRef]
46. Xu, C.; Yang, B.; Zhang, R.; Li, Z.; Wu, Q. Basin-Forming Mechanism, Basin Geodynamic and Hydrocarbon Exploration of the South Yellow Sea Rift Basin, East Asia: New Insights From Tectono-Thermal Evolution and Geophysical Data. *Geol. J.* **2025**, *60*, 2530–2560. [CrossRef]
47. Shi, Z.; Wei, P.; Wang, L.; Xue, L.; Pang, W.; Chen, B.; Ma, L.; Shi, J.; Zhao, Y. Formation of the stratigraphic hydrocarbon accumulations of the Upper Yabus Formation in the Northern Sub-basin of the Melut Basin, South Sudan. *J. Afr. Earth Sci.* **2021**, *177*, 104166. [CrossRef]

48. Yang, Z.; Wu, D.; Bao, H.; Li, W.; Wei, L.; Ma, Z.; Ren, J.; Wang, Q.; Zhang, H. Near-source exploration progress and reflections of marine gas-bearing system in the Ordovician carbonate–gypsum-salt rock strata in the Ordos Basin, NW China. *Pet. Explor. Dev.* **2026**, *53*, 372–385. [CrossRef]
49. Huo, X.; Chen, J.; Wu, Q.; Chen, C.; Pang, H.; Liu, X.; Jiang, F.; Tian, Z. Origin and migration-accumulation characteristics of hydrocarbons in Paleozoic-Proterozoic buried hills of the Shuguang area, Western Sag, Liaohe depression. *Carbonates Evaporites* **2025**, *40*, 142. [CrossRef]
50. Gao, Y.; Liu, H. Geological characteristics and hydrocarbon accumulation model of the whole petroleum system in Paleogene of Jiyang Depression, Bohai Bay Basin, China. *Pet. Explor. Dev.* **2025**, *52*, 616–629. [CrossRef]
51. Ji, T.; Yang, W.; Wu, X.; Li, D.; Liu, M.; Song, C.; Chen, X. Sedimentary characteristics, lithofacies, and paleogeography of the Middle–Lower Cambrian in the Tarim Basin, NW China. *Can. J. Earth Sci.* **2024**, *61*, 560–585. [CrossRef]
52. Zhu, Y.; Zheng, J.; Li, L.; Fe, G.; Wu, F.; Ya, L.; Zhang, T. Lithofacies paleogeography and exploration significance of lower cambrian wusonger formation depositional stage, Tarim Basin, NW China. *Nat. Gas Geosci.* **2022**, *33*, 1–12.
53. Cardott, B.J.; Comer, J.B. *Woodford Shale (Upper Devonian to Lower Mississippian): From Hydrocarbon Source Rock to Reservoir*; University of Oklahoma: Norman, OK, USA, 2021.
54. Mülayim, O. *Cenomanian–Turonian Platform Evolution and Records of OAE 2 on the Drowned Northern Arabian Carbonate Platform (SE Turkey): Integration of Biostratigraphy, Sequence Stratigraphy, Sedimentology, and Stable Isotopes*; Middle East Technical University (Turkey): Ankara, Turkey, 2020.
55. Cheng, W.; Wang, R.; He, T.; Sun, C.; Tian, H.; Zhao, J.; Zhao, Y.; He, J.; Zeng, Q.; Liu, J. Geochemical evidence of organic matter enrichment and depositional dynamics in the lower cambrian yurtus Formation, NW Tarim basin: Insights into hydrothermal influence and paleoproductivity mechanisms. *Minerals* **2025**, *15*, 288. [CrossRef]
56. Li, Y.; Fan, T.; Shi, J.; Jiang, M.; Zhang, T.; Kuang, M.; Liu, W. Evolution of Deep Marine Sedimentary Filling and Development of High-Quality Hydrocarbon Source Rocks in Cratonic Basins, China. In *Petroleum Geology and Exploration of Deep Marine Strata in China*; Springer: Berlin/Heidelberg, Germany, 2026; pp. 35–56.
57. Zhu, Y.; Zheng, J.; Zhang, J.; Luo, X.; Yu, G.; Li, J.; Hu, F.; Yang, G. Facies, depositional environment and reservoir quality of an early Cambrian carbonate ramp in the Tarim Basin, NW China. *Minerals* **2023**, *13*, 791. [CrossRef]
58. Tan, X.; Li, L.; Liu, H.; Luo, B.; Zhou, Y.; Wu, J.; Ding, X. General depositional features of the carbonate platform gas reservoir of the Lower Triassic Jialingjiang Formation in the Sichuan Basin of southwest China: Moxi gas field of the central basin. *Carbonates Evaporites* **2011**, *26*, 339–350. [CrossRef]
59. Shen, A.; Zheng, J.; Chen, Y.; Ni, X.; Huang, L. Characteristics, origin and distribution of dolomite reservoirs in Lower-Middle Cambrian, Tarim Basin, NW China. *Pet. Explor. Dev.* **2016**, *43*, 375–385. [CrossRef]
60. Latif, K.; Xiao, E.; Riaz, M.; Wang, L.; Khan, M.Y.; Hussein, A.A.; Khan, M.U. Sequence stratigraphy, sea-level changes and depositional systems in the Cambrian of the North China Platform: A case study of Kouquan section, Shanxi Province, China. *J. Himal. Earth Sci.* **2018**, *51*, 1–16.
61. Goldhammer, R.; Dunn, P.; Hardie, L. Depositional cycles, composite sea-level changes, cycle stacking patterns, and the hierarchy of stratigraphic forcing: Examples from Alpine Triassic platform carbonates. *GSA Bull.* **1990**, *102*, 535–562. [CrossRef]
62. Chen, D.; Tucker, M.E. The Frasnian–Famennian mass extinction: Insights from high-resolution sequence stratigraphy and cyclostratigraphy in South China. *Palaeogeogr. Palaeoclim. Palaeoecol.* **2003**, *193*, 87–111. [CrossRef]
63. Glumac, B. Cessation of Grand Cycle Deposition in the Framework of Passive Margin Evolution: Controlling Mechanisms and Effects on Carbonate Deposition and Diagenesis, Cambrian Maynardville Formation, Southern Appalachians. Ph.D. Thesis, The University of Tennessee, Knoxville, TN, USA, 1997.
64. Collins, L. Geological setting, marine geomorphology, sediments and oceanic shoals growth history of the Kimberley region. *J. R. Soc. West. Aust.* **2011**, *94*, 89.
65. Gao, Z.; Fan, T. Carbonate platform-margin architecture and its influence on Cambrian-Ordovician reef-shoal development, Tarim Basin, NW China. *Mar. Pet. Geol.* **2015**, *68*, 291–306. [CrossRef]
66. Pfeil, R.; Read, J. Cambrian carbonate platform margin facies, Shady Dolomite, southwestern Virginia, USA. *J. Sediment. Res.* **1980**, *50*, 91–116. [CrossRef]
67. Rees, M. A fault-controlled trough through a carbonate platform: The Middle Cambrian House Range embayment. *GSA Bull.* **1986**, *97*, 1054–1069. [CrossRef]
68. Sun, S.Q.; Esteban, M. Paleoclimatic controls on sedimentation, diagenesis, and reservoir quality: Lessons from Miocene carbonates. *AAPG Bull.* **1994**, *78*, 519–543. [CrossRef]
69. Han, C.; Lin, C.; Wei, T.; Dong, C.; Ren, L.; Zhang, X.; Dong, L.; Zhao, X. Paleogeomorphology restoration and the controlling effects of paleogeomorphology on karst reservoirs: A case study of an ordovician-aged section in Tahe oilfield, Tarim Basin, China. *Carbonates Evaporites* **2019**, *34*, 31–44. [CrossRef]
70. Shen, A.; Zhao, W.; Hu, A.; She, M.; Chen, Y.; Wang, X. Major factors controlling the development of marine carbonate reservoirs. *Pet. Explor. Dev.* **2015**, *42*, 597–608. [CrossRef]

71. Zhang, J.; Zhou, J.; Fu, L.; Li, H.; Lou, D.J. Karstification of Ordovician carbonate reservoirs in Huanghua depression and its control factors. *Carbonates Evaporites* **2020**, *35*, 42. [CrossRef]
72. Xie, J.; Guo, G.a.; Tang, Q.; Peng, X.; Deng, H.; Xu, W. Key technologies for the efficient development of ultra-deep ancient dolomite karst gas reservoirs: A case study of the Sinian Dengying Formation gas reservoir in the Anyue Gas Field of the Sichuan Basin. *Nat. Gas Ind. B* **2021**, *8*, 588–595. [CrossRef]
73. Macurda, D.B. *Carbonate Seismic Facies Analysis*; Society of Exploration Geophysicists: Alief, TX, USA, 1997.
74. Anselmetti, F.S.; Eberli, G.P.; Bernoull, D. Seismic modeling of a carbonate platform margin (Montagna della Maiella, Italy): Variations in seismic facies and implications for sequence stratigraphy. In *Carbonate Seismology*; Society of Exploration Geophysicists: Alief, TX, USA, 1997.
75. Embry, J.-C.; Hunt, D.W.; Colpaert, A.; Dræge, A.; Zahm, L. Seismic facies, stratigraphy, geomorphology, and seismic modelling of a Lower Cretaceous carbonate platform. *Geol. Soc.* **2021**, *509*, 89–104. [CrossRef]
76. Sellwood, B.W. Principles of carbonate diagenesis. In *Quantitative Diagenesis: Recent Developments and Applications to Reservoir Geology*; Springer: Berlin/Heidelberg, Germany, 1994; Volume 453, pp. 1–32.
77. Yang, L.; Chen, D.; Hu, J.; Meng, X.; Liu, J.; Yang, W. Understanding the role of sequence stratigraphy and diagenesis on the temporal and spatial distribution of carbonate reservoir quality: A conceptual modeling approach. *Mar. Pet. Geol.* **2023**, *147*, 106010. [CrossRef]
78. Maliva, R.G. Carbonate facies models and diagenesis. In *Aquifer Characterization Techniques*; Schlumberger Methods in Water Resources Evaluation Series No. 4; Springer: Berlin/Heidelberg, Germany, 2016; pp. 91–110.
79. Nader, F.H. *Multi-Scale Quantitative Diagenesis and Impacts on Heterogeneity of Carbonate Reservoir Rocks*; Springer: Berlin/Heidelberg, Germany, 2017.
80. Liu, Y.; Feng, J.; Xu, W.; Zhang, T.; Jing, Y.; Wang, H. Characteristics of strike slip faults and their control on dolomite gas reservoirs in Gucheng area, Tarim Basin. *China Pet. Explor.* **2022**, *27*, 135–148.
81. Dorobek, S.L. Tectonic and depositional controls on syn-rift carbonate platform sedimentation. In *Controls on Carbonate Platform and Reef Development*; SEPM, Society for Sedimentary Geology: Tulsa, OK, USA, 2008.
82. Cross, N.E.; Bosence, D.W. Tectono-sedimentary models for rift-basin carbonate systems. In *Controls on Carbonate Platform and Reef Development*; SEPM, Society for Sedimentary Geology: Tulsa, OK, USA, 2008.
83. Bosence, D.; Cross, N.; Hardy, S. Architecture and depositional sequences of Tertiary fault-block carbonate platforms; an analysis from outcrop (Miocene, Gulf of Suez) and computer modelling. *Mar. Pet. Geol.* **1998**, *15*, 203–221. [CrossRef]
84. Cen, Y.; Tang, Q.; Li, J.; Liang, F.; Zhang, X.; Wang, L.; Liu, Q.; Li, H. Controlling effect of strike-slip faults on Ediacaran Dengying Formation microbial mound-shoal complex reservoir, Penglai Gas Field, SW China. *Appl. Earth Sci. Trans. Inst. Min. Metall.* **2025**, *135*, 210–225. [CrossRef]
85. Chen, X.; Satti, I.; Dong, Y. Microfacies, geometry and growth phases of microbial mound in Gucheng area, Southeastern Tarim Basin, China. *Turk. J. Earth Sci.* **2024**, *33*, 99–117. [CrossRef]
86. Read, J. Carbonate platform facies models. *AAPG Bull.* **1985**, *69*, 1–21. [CrossRef]
87. Pomar, L.J. Types of carbonate platforms: A genetic approach. *Basin Res.* **2001**, *13*, 313–334. [CrossRef]
88. Read, J. Carbonate platforms of passive (extensional) continental margins: Types, characteristics and evolution. *Tectonophysics* **1982**, *81*, 195–212. [CrossRef]
89. Berra, F.; Carminati, E.; Jadoul, F.; Binda, M. Does compaction-induced subsidence control accommodation space at the top of prograding carbonate platforms? Constraints from the numerical modelling of the Triassic Esino Limestone (Southern Alps, Italy). *Mar. Pet. Geol.* **2016**, *78*, 621–635. [CrossRef]
90. Paterson, R.J.; Whitaker, F.F.; Jones, G.D.; Smart, P.L.; Waltham, D.; Felce, G. Accommodation and sedimentary architecture of isolated icehouse carbonate platforms: Insights from forward modeling with CARB3D+. *J. Sediment. Res.* **2006**, *76*, 1162–1182. [CrossRef]
91. Husson, L.; Pastier, A.M.; Pedoja, K.; Elliot, M.; Paillard, D.; Authemayou, C.; Sarr, A.C.; Schmitt, A.; Cahyarini, S.Y. Reef carbonate productivity during quaternary sea level oscillations. *Geochem. Geophys. Geosystems* **2018**, *19*, 1148–1164. [CrossRef]
92. Xiao, Y.; Whitaker, F.; Al-Helal, A.; Stafford, S.; Gomez-Rivas, E.; Guidry, S. Fundamental approaches to dolomitization and carbonate diagenesis in different hydrogeological systems and the impact on reservoir quality distribution. In Proceedings of the IPTC 2013: International Petroleum Technology Conference, Beijing, China, 26–28 March 2013; p. cp–350-00111.
93. Li, J.; Wei, P.; Shi, L.; Chen, G.; Peng, W.; Sun, S.; Zhang, B.; Xie, M.; Hong, L. Fluid interaction mechanism and diagenetic reformation of basement reservoirs in Beier Sag, Hailar Basin, China. *Pet. Explor. Dev.* **2020**, *47*, 46–58. [CrossRef]
94. Smeraglia, L.; Berra, F.; Billi, A.; Boschi, C.; Carminati, E.; Doglioni, C. Origin and role of fluids involved in the seismic cycle of extensional faults in carbonate rocks. *Earth Planet. Sci. Lett.* **2016**, *450*, 292–305. [CrossRef]
95. Tian, W.; Jiang, T.; Wu, G.; Yang, S.; Zhang, Y.; Ma, B.; Qiu, C.; Sun, C. Key controls on the formation of reservoirs along the ultra-deep strike-slip fault zone in the depression of the northern Tarim Basin, NW China. *Pet. Explor. Dev.* **2025**, *52*, 1527–1537. [CrossRef]

96. Yu, J.; Shi, K.; Wang, Q.; Liu, B.; Han, J.; Song, Y.; Kong, Y.; Jiang, W. Structural diagenesis of deep carbonate rocks controlled by intra-cratonic strike-slip faulting: An example in the Shunbei area of the Tarim Basin, NW China. *Basin Res.* **2022**, *34*, 1601–1631. [CrossRef]
97. Yao, Y.; Zeng, L.; Mao, Z.; Song, Y.; Tan, X.; Lin, B.; Liu, G.; Cao, D.; Ostadhassan, M.; Zhang, Q. Strike-slip Fault Architecture and its Control on Fractured Carbonate Reservoirs: Insight from Outcrops in the North-western Tarim Basin, NW China. *Acta Geol. Sin.* **2025**, *99*, 568–581. [CrossRef]
98. Bádenas, B.; Aurell, M.J.F. Facies models of a shallow-water carbonate ramp based on distribution of non-skeletal grains (Kimmeridgian, Spain). *Facies* **2010**, *56*, 89–110. [CrossRef]
99. Moore, C.H. *Carbonate Diagenesis and Porosity*; Elsevier: Amsterdam, The Netherlands, 1989; Volume 46.
100. Rao, V.P.; Gopinathan, P. Late Quaternary sediments on the carbonate platform off western India: Analogues of ancient platform carbonates. *J. Earth Syst. Sci.* **2019**, *128*, 80. [CrossRef]
101. Gao, Z.; Ding, Q.; Hu, X. Characteristics and controlling factors of carbonate intra-platform shoals in the Tarim Basin, NW China. *J. Pet. Sci. Eng.* **2015**, *127*, 20–34. [CrossRef]
102. Xia, M.; Zhang, B.; Jia, S.; Zhao, C.; Feng, M.; Shang, J.; Zhang, C.; Li, Y.; Li, Y. Retrogradation of carbonate platforms on a rifted margin: The late Ediacaran record of the northwestern Yangtze Craton (SW China). *Front. Earth Sci.* **2024**, *12*, 1401426. [CrossRef]
103. Bao, H.; Zheng, Z.; Xu, G.; Li, R.; Wang, Q.; Saafi, M.; Ye, J. Performance and mechanism of sand stabilization via microbial-induced CaCO3 precipitation using phosphogypsum. *J. Clean. Prod.* **2024**, *468*, 142999. [CrossRef]
104. Mai, Z.; Chen, Q.; Wang, L.; Zhang, J.; Cheng, H.; Su, H.; Zhang, S.; Li, J. Bacterial carbonic anhydrase-induced carbonates mitigate soil erosion in biological soil crusts. *J. Environ. Manag.* **2024**, *352*, 120085. [CrossRef] [PubMed]
105. Zhang, K.; Tang, C.-S.; Jiang, N.-J.; Pan, X.-H.; Liu, B.; Wang, Y.-J.; Shi, B. Microbial-induced carbonate precipitation (MICP) technology: A review on the fundamentals and engineering applications. *Environ. Earth Sci.* **2023**, *82*, 229. [CrossRef] [PubMed]
106. Minisini, D.; Simo, T.; Macquaker, J.H.; Rudnicki, M.D. Controls on storage capacity in mudstones. Cementation before sediment compaction and preservation of porosity in lithified rock. *Mar. Pet. Geol.* **2025**, *177*, 107350. [CrossRef]
107. Wang, S.; Yang, X.; Lu, Y.; Su, P.; Liu, D.; Meng, L.; Wang, Q.; Li, L.; Radwan, A.E. Densification mechanism of deep low-permeability sandstone reservoir in deltaic depositional setting and its implications for resource development: A case study of the Paleogene reservoirs in Gaoshangpu area of Nanpu sag, China. *Front. Earth Sci.* **2022**, *10*, 996167. [CrossRef]
108. Fan, A.; Yang, R.; Lenhardt, N.; Wang, M.; Han, Z.; Li, J.; Li, Y.; Zhao, Z. Cementation and porosity evolution of tight sandstone reservoirs in the Permian Sulige gas field, Ordos Basin (central China). *Mar. Pet. Geol.* **2019**, *103*, 276–293. [CrossRef]
109. Sun, M.; Yensepbayev, T.; Zhanserkeyeva, A.; Abylay, A. Elemental Geochemistry, Paleoproductivity Variations and Their Controlling Factors of Lower Cambrian Organic-Rich Strata in the Tarim Basin. *Geosciences* **2026**, *16*, 258. [CrossRef]
110. Talebi, E.; Mehrabi, H.; Honarmand, J. Microporous mud-dominated facies in Upper Cretaceous carbonate sequences of the Abadan Plain, SW Iran: Depositional model, diagenesis history and petrophysical properties. *Facies* **2025**, *71*, 16. [CrossRef]
111. Müller-Huber, E.; Börner, F.; Börner, J.H.; Kulke, D. Combined interpretation of NMR, MICP, and SIP measurements on mud-dominated and grain-dominated carbonate rocks. *J. Appl. Geophys.* **2018**, *159*, 228–240. [CrossRef]
112. Machel, H.G. Investigations of burial diagenesis in carbonate hydrocarbon reservoir rocks. *Geosci. Can.* **2005**, *32*, 103–128.
113. Wolf, K.H.; Chilingarian, G. Diagenesis of sandstones and compaction. In *Developments in Sedimentology*; Elsevier: Amsterdam, The Netherlands, 1975; pp. 64–444.
114. Tada, R.; Siever, R. Pressure solution during diagenesis. *Ann. Rev. Earth Planet. Sci.* **1989**, *17*, 89. [CrossRef]
115. Ehrenberg, S.; Eberli, G.; Keramati, M.; Moallemi, S.A. Porosity-permeability relationships in interlayered limestone-dolostone reservoirs. *AAPG Bull.* **2006**, *90*, 91–114. [CrossRef]
116. Kaczmarek, S.E.; Sibley, D.F. Direct physical evidence of dolomite recrystallization. *Sedimentology* **2014**, *61*, 1862–1882. [CrossRef]
117. Malone, M.J.; Baker, P.A.; Burns, S.J. Recrystallization of dolomite: An experimental study from. *Geochim. Cosmochim. Acta* **1996**, *60*, 2189–2207. [CrossRef]
118. Malone, M.J.; Baker, P.A.; Burns, S.J. Recrystallization of dolomite: Evidence from the Monterey Formation (Miocene), California. *Sedimentology* **1994**, *41*, 1223–1239. [CrossRef]
119. Ledbetter Ferrill, N.S.; Li, X.; Tesauro, J.; Sears, M.; Bradley, G.M.; Hilbert, A.; Carney, E.; Saxby, J.; Mobasher, N.; Kelley, B.M. Massive Dolomitization of Interior and Slope to Basin-Margin Facies of the Triassic Yangtze Platform Through Superposed Earth-Surface and Burial Mechanisms, Nanpanjiang Basin, South China. *Minerals* **2025**, *15*, 324. [CrossRef]
120. Gao, J.; Zheng, H.; Liu, B.; Pan, L.; Li, R.; Wu, J.; Yang, X.; Tang, H.; Dong, Y. Genetic Mechanism of Structurally Controlled Dolomites Derived from Seawater-Hydrothermal Mixed Fluids—A Case Study from Middle Permian, Central Sichuan Basin, South China. *Minerals* **2023**, *13*, 758. [CrossRef]
121. Milroy, P.; Wright, V.J. Fabrics, facies control and diagenesis of lacustrine ooids and associated grains from the Upper Triassic, southwest England. *Geol. J.* **2002**, *37*, 35–53. [CrossRef]
122. Dawson, W.C.; Carozzi, A.V.J. Experimental deep burial, fabric-selective dissolution in Pennsylvanian phylloid algal limestones. *Carbonates Evaporites* **1993**, *8*, 71–81. [CrossRef]

123. Flügel, E. Diagenesis, porosity, and dolomitization. In *Microfacies of Carbonate Rocks: Analysis, Interpretation and Application*; Springer: Berlin/Heidelberg, Germany, 2004; pp. 267–338.
124. Xiong, Y.; Tan, X.; Zuo, Z.; Zou, G.; Liu, M.; Liu, Y.; Liu, L.; Xiao, D.; Zhang, J. Middle Ordovician multi-stage penecontemporaneous karstification in North China: Implications for reservoir genesis and sea level fluctuations. *J. Asian Earth Sci.* **2019**, *183*, 103969. [CrossRef]
125. Zhang, Y.-f.; Wang, Z.-y.; Qu, H.-z.; Luo, C.-s.; Li, Y. Sedimentary microtopography in sequence stratigraphic framework of Upper Ordovician and its control over penecontemporaneous karstification, No. I slope break, Tazhong, Tarim block. *J. Cent. South Univ.* **2014**, *21*, 735–744. [CrossRef]
126. Cheng, Y.; Liu, J.; Meng, Q.; Yang, Y. Characteristics and controlling factors of the unconformity-related carbonate reservoir: A case study from Sinian Shuiquan Formation, Tarim Basin, northwestern China. *Aust. J. Earth Sci.* **2024**, *71*, 423–438. [CrossRef]
127. Zhang, B.; Liu, J. Classification and characteristics of karst reservoirs in China and related theories. *Pet. Explor. Dev.* **2009**, *36*, 12–29. [CrossRef]
128. Wei, W.; Chen, D.; Qing, H.; Qian, Y. Hydrothermal dissolution of deeply buried Cambrian dolomite rocks and porosity generation: Integrated with geological studies and reactive transport modeling in the Tarim Basin, China. *Geofluids* **2017**, *2017*, 9562507. [CrossRef]
129. Fyfe, W.S. *Fluids in the Earth's Crust: Their Significance in Metamorphic, Tectonic and Chemical Transport Process*; Elsevier: Amsterdam, The Netherlands, 2012; Volume 1.
130. Chen, L.; Ji, H.; Zhang, L.; Jia, H.; Zhu, Y.; Fang, Z. Effect of burial processes on the evolution of organic acids and implications for acidic dissolution from a case study of the Nanpu Sag, Bohai Bay Basin, China. *J. Nat. Gas. Sci. Eng.* **2017**, *39*, 173–187. [CrossRef]
131. Su, J.; Wang, X.; Yang, H.; Yu, F.; Li, Y.; Ma, S.; Wei, C.; Weng, N.; Yang, Y. Hydrothermal alteration and hydrocarbon accumulations in ultra-deep carbonate reservoirs along a strike-slip fault system, Tarim Basin, NW China. *J. Pet. Sci. Eng.* **2021**, *203*, 108605. [CrossRef]
132. Zeng, L.; Song, Y.; Han, J.; Han, J.; Yao, Y.; Huang, C.; Zhang, Y.; Tan, X.; Li, H. Control of structure and fluid on ultra-deep fault-controlled carbonate fracture-vug reservoirs in the Tarim Basin, NW China. *Pet. Explor. Dev.* **2025**, *52*, 143–156. [CrossRef]
133. Liu, Z.; Wu, K.; Wang, B.; Zhang, H.; Xu, K.; Wang, K. Evaluation of Fracture Effectiveness in Ultra-Deep Marine Carbonate Reservoirs of Fuman Oilfield, Tarim Basin. *Appl. Sci.* **2026**, *16*, 2511. [CrossRef]
134. Roure, F.; Swennen, R.; Schneider, F.; Faure, J.; Ferket, H.; Guilhaumou, N.; Osadetz, K.; Robion, P.; Vandeginste, V. Incidence and importance of tectonics and natural fluid migration on reservoir evolution in foreland fold-and-thrust belts. *Oil Gas Sci. Technol.* **2005**, *60*, 67–106. [CrossRef]
135. Wang, J.; Wang, H.; Zhang, R.; Dong, L.; Wang, K.; Zhang, Z. Improvement of reservoir quality of ultra-deep tight sandstones by tectonism and fluid: A case study of Keshen gas field in Tarim Basin, western China. *Petroleum* **2023**, *9*, 124–134. [CrossRef]
136. Li, K.; Zhu, L.; Xiong, F.; Liu, J.; Xue, Y.; Cao, Z.; Zhou, Y.; Liang, X.; Ji, M.; Liu, G.; et al. Review on Thermal Stimulation in Deep Geothermal Reservoirs: Thermo-Mechanical Mechanisms and Fracture Evolution. *Processes* **2026**, *14*, 1199. [CrossRef]
137. Lu, X.; Wang, Y.; Tian, F.; Li, X.; Yang, D.; Li, T.; Lv, Y.; He, X. New insights into the carbonate karstic fault system and reservoir formation in the Southern Tahe area of the Tarim Basin. *Mar. Pet. Geol.* **2017**, *86*, 587–605. [CrossRef]
138. Wu, G.; Yang, H.; He, S.; Cao, S.; Liu, X.; Jing, B. Effects of structural segmentation and faulting on carbonate reservoir properties: A case study from the Central Uplift of the Tarim Basin, China. *Mar. Pet. Geol.* **2016**, *71*, 183–197. [CrossRef]
139. Tian, F.; Luo, X.; Zhang, W. Integrated geological-geophysical characterizations of deeply buried fractured-vuggy carbonate reservoirs in Ordovician strata, Tarim Basin. *Mar. Pet. Geol.* **2019**, *99*, 292–309. [CrossRef]
140. Wang, Y.; Chen, H.; Liu, Y.; Wang, S.; Han, C.; Li, Z.; Ma, Y. The Structural and Diagenetic Coupling Controls the Distribution of Deep Carbonate Rock Reservoirs in the Southern of Tahe Oilfield, Tarim Basin. *Geosciences* **2025**, *15*, 435. [CrossRef]
141. Lee, E.Y.; Kominz, M.; Reuning, L.; Gallagher, S.J.; Takayanagi, H.; Ishiwa, T.; Knierzinger, W.; Wagreich, M. Quantitative compaction trends of Miocene to Holocene carbonates off the west coast of Australia. *Aust. J. Earth Sci.* **2021**, *68*, 1149–1161. [CrossRef]
142. Rivers, J.M.; Dalrymple, R.W. The reconstruction of coastal carbonate sequence stratigraphy: A modern-systems approach. *Geology* **2025**, *53*, 232–237. [CrossRef]
143. Hidayat, R.; Murray-Wallace, C.V.; Jacobs, Z.J. Late Pleistocene evolution of Robe Range, southern Australia–The timing and carbonate source dynamics of coastal dune development. *Mar. Geol.* **2023**, *456*, 106987. [CrossRef]
144. Mory, A.; Mantle, D.; Backhouse, J. Revisiting Upper Permian Stratigraphy, Northern Perth Basin, Western Australia. *J. R. Soc. West. Aust.* **2025**, *108*. [CrossRef]
145. Zhao, S.; Chen, W.; Sun, J.; Shen, Z.; Zhang, J. Mesozoic–Cenozoic Thermochronology of the Tarim–Southern Tianshan System, NW China. *Geol. J.* **2025**, *61*, 2258–2278. [CrossRef]
146. Deng, X.; Bai, B. Whole petroleum system and main controlling factors of hydrocarbon accumulation in the Mesozoic of Ordos Basin, NW China. *Pet. Explor. Dev.* **2025**, *52*, 1150–1163. [CrossRef]

147. Li, J.; Yang, X.; Dong, C.; Li, J.; Xu, Z.; Zhang, L.; Zhang, W. Characteristics of orderly hydrocarbon accumulation of deep reservoirs in Kuqa Depression and its exploration implications. *Geol. J.* **2023**, *58*, 4103–4120. [CrossRef]
148. Lan, Z.; Shen, J. Depositional paleo-environments of Lower Cambrian Qiongzhusi Formation in the Western Middle Yangtze Block and its controlling effect on the organic matter enrichment. *Energies* **2022**, *15*, 3761. [CrossRef]
149. Luo, J.; Zhang, T.; Min, H.; Shu, H.; Zhang, Z.; Zhang, X. Sedimentary environment evolution and organic matter enrichment mechanisms of the cambrian Qiongzhusi Formation in the southwestern Yangtze Block. *Sci. Rep.* **2026**, *16*, 9294. [CrossRef] [PubMed]
150. Lundegard, P.D.; Johnson, P.C. Source zone natural attenuation at petroleum hydrocarbon spill sites—II: Application to a former oil field. *Groundw. Monit. Remediat.* **2006**, *26*, 93–106. [CrossRef]
151. Zhang, H.; Wang, X.; Zhao, X.; Pu, M.; Lü, X. Evolution of the Hydrocarbon Migration System in the Western Region of the Kuqa Foreland Basin. *Appl. Sci.* **2026**, *16*, 1591. [CrossRef]
152. Zhang, F.; Chen, Z.; Lu, X.; Ru, R.; Zhang, W.; Tian, J.; Yin, S. Effect of Overpressure on Porosity of Deep Reservoirs in a Compressive Setting based on Numerical Simulations: A Case Study of the Lower Cretaceous Bashijiqike Formation in the Kuqa Foreland Basin, Tarim Basin, NW China. *Acta Geol. Sin.* **2025**, *99*, 1819–1835. [CrossRef]
153. Li, W.; Yu, Z.; Wang, X.; Yu, Z.; Lu, X.; Feng, Q. Formation mechanisms of deep and ultra-deep over pressure caprocks and their relationships with super-large gas fields in the petroliferous basins of China. *Nat. Gas Ind. B* **2020**, *7*, 443–452. [CrossRef]
154. Xu, K.; Yang, H.; Zhang, H.; Ju, W.; Li, C.; Fang, L.; Wang, Z.; Wang, H.; Yuan, F.; Zhao, B.; et al. Fracture effectiveness evaluation in ultra-deep reservoirs based on geomechanical method, Kuqa Depression, Tarim Basin, NW China. *J. Pet. Sci. Eng.* **2022**, *215*, 110604. [CrossRef]
155. Hao, F. Enrichment mechanism and prospects of deep oil and gas. *Acta Geol. Sin.* **2022**, *96*, 742–756. [CrossRef]
156. Ding, Z.; Wang, R.; Chen, F.; Yang, J.; Zhu, Z.; Yang, Z.; Sun, X.; Xian, B.; Li, E.; Shi, T.; et al. Origin, hydrocarbon accumulation and oil-gas enrichment of fault-karst carbonate reservoirs: A case study of Ordovician carbonate reservoirs in South Tahe area of Halahatang oilfield, Tarim Basin. *Pet. Explor. Dev.* **2020**, *47*, 306–317. [CrossRef]
157. He, J.; Li, H.; Luo, L.; Qiao, L.; Li, J.; Ma, X.; Zhang, Y.; Yao, J.; Jiang, S.; Wang, Y. Controlling Mechanisms of Burial Karstification in Gypsum Moldic Vug Reservoirs of the 4-1 Sub-Member, Member 5 of the Majiagou Formation, Central Ordos Basin. *Processes* **2026**, *14*, 275. [CrossRef]
158. Zhang, J.; Zhang, Y.; Li, Y.; Ni, C.; Zhong, J.; Li, H.; Chen, Y.; Yuan, Q. The Critical Factors in the Formation of Ultra-Deep Carbonate Reservoirs: A Case Study of Tarim Basin and Sichuan Basin, Midwest China. *Geol. J.* **2026**, *11*, 287–299. [CrossRef]

Disclaimer/Publisher's Note: The statements, opinions and data contained in all publications are solely those of the individual author(s) and contributor(s) and not of MDPI and/or the editor(s). MDPI and/or the editor(s) disclaim responsibility for any injury to people or property resulting from any ideas, methods, instructions or products referred to in the content.